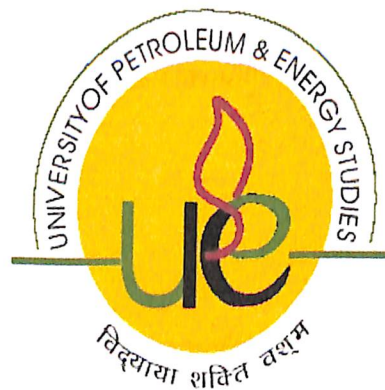


MODELING AND SIMULATION OF PERMANENT MAGNET  
GENERATOR AND INVERTER FOR SMALL SCALE WIND  
POWER GENERATION USING MATLAB/SIMULINK

By  
Siddhaling Ganer



College of Engineering  
University of Petroleum & Energy Studies  
Dehradun  
Apr, 2013

# MODELING AND SIMULATION OF PERMANENT MAGNET GENERATOR AND INVERTER FOR SMALL SCALE WIND POWER GENERATION USING MATLAB/SIMULINK

A thesis submitted in partial fulfilment of the requirements for the Degree of  
Master of Technology  
(Energy Systems)

By  
Siddhaling Ganer

Under the guidance of

**Mr. AGAM KUMAR TYAGI**  
*Assistant Professor, Electrical Engg department*  
*University Of Petroleum and Energy Studies*  
*Dehradun.*

Approved

.....  
Dean

College of Engineering  
University of Petroleum & Energy Studies  
Dehradun  
Apr, 2013

## CERTIFICATE

This is to certify that the work contained in this thesis titled "MODELING AND SIMULATION OF PERMANENT MAGNET GENERATOR AND INVERTER FOR SMALL SCALE WIND POWER GENERATION USING MATLAB/SIMULINK" has been carried out by **Siddhaling Ganer** under my/our supervision and has not been submitted elsewhere for a degree.

*Aty*  
*25/04/13*

**Mr. AGAM KUMAR TYAGI**  
*Assistant Professor, Electrical Engg department*  
*University Of Petroleum and Energy Studies*  
*Dehradun.*  
22-April-2013

## ABSTRACT

In the last years, a rising interest in non-contaminant energy source has emerged from the industrial and academic communities. Major RES, i.e. wind and solar are today economically feasible alternatives to conventional electric power generation. Among the various factors contributing to this success are the development of new technologies, new circuit topologies and novel control strategies.

Research on performance improvement of and cost reduction in such non-conventional energy conversion systems is being accorded the highest priority. Wind power generation has a strong connection to rotating machinery and hence its practical application is most promising. Wind generator control methods have been already proposed to efficiently utilize the wind power which is prone to fluctuation every moment. The induction type machine has the advantage of robustness, low cost and maintenance-free operation. However they have drawback of low power factor and need for an AC excitation source. Permanent magnet generator is chosen so as to eliminate the drawbacks of induction generator. Boost chopper circuit with a single switching device is choice for power control and provides an improved efficiency.

In this report we discuss about the permanent magnet generator and its characteristics. This report contains various sections each section describe specific region. Permanent Magnet Generator consists of synchronous Machine, Uncontrolled Rectifier, DC-Power storage, PWM Inverter, Load Side Filter (LSF).

Finally, Permanent Magnet Generator (PMG) simulate in Matlab Environment to study its characteristics in different torque condition. In this report contains Steady state analysis of the PMGG, which makes easy to understand, how wind speed, power, torque etc. By providing a brief description of Rectifier and PWM Inverter, which is simulated in Matlab; make us easy to understand, how electrical element works.

## ACKNOWLEDGEMENT

I am thankful to College of Engineering Studies at University of Petroleum and Energy Studies to carry out this project.

I would like to express my gratitude to Mr. Agam Kumar Tyagi for help, inspiration, encouragement and his continuous guidance throughout this work. I would also like to thank my examiner Prof. Madhu Sharma for valuable comments and encouragement.

I would like to thank my parents for their lifetime support, generous love, never-ending patience, and inspiration. Finally, I am thankful to my friends for their valuable time and support.

## List of Figures:

Fig. 1.1 A range of small wind turbines	3
Fig. 1.2 Power Curve for the 10 kW Bergey BWC Turbine	7
Fig. 1.3 Power curve for the Vestas V80 turbine	8
Fig. 1.4 Power coefficient variation with tip speed ratio for the Vestas V80	9
Fig. 2.1: Small turbine system with basic circuit breaker and switch protection	11
Fig. 3.1 Over-speeding of the Aerogenesis 5 kW wind turbine	19
Fig. 3.2 Outside and inside views of the Ginlong 500-A PMG.	20
Fig. 3.3 Schematic of a PMG wind turbine feeding the grid	22
Fig. 3.4 Schematic of a 3-phase diode rectifier	23
Fig. 3.6 A simple single phase full-bridge inverter	25
Fig. 3.7 Modified square wave load voltage waveform for a single-phase inverter without a filter	25
Fig. 4.1 Model of Permanent Magnet Generator	31
Fig. 4.2 Waveforms of output voltages of permanent magnet generator	32
Fig. 4.3 Model of Three-phase full-wave rectifier	33
Fig. 4.4 Voltage waveform across diodes D1 and D2 and input supply	34
Fig. 4.5 Current and voltage waveform for the resistive load	34
Fig. 4.6 Model of Boost Chopper	36
Fig. 4.7 Waveforms of the load voltage, load current, and current through the inductor	36
Fig. 4.8 PWM pulse generator	38
Fig. 4.10 Waveforms of gate pulse, current through M1, and output voltage	39

Fig. 4.11 Output Filters	39
Fig. 4.13 Complete model of PMG	41
Fig. 4.14 Output of the inverter before filtering	42
Fig. 4.15 Output of the inverter after filtering	42

### List of Tables:

Table.1.1 Power and power coefficient variation with wind speed for the Vestas V80 2 MW and Bergey XL 10 kW turbines	9
Table 2.1. Change of Duty Ratio of Chopper with respect to Wind Velocity	15
Table 3.1 Main parameters of the Ginlong 500-A PMG	21

## NOMENCLATURE

$A_r$  = swept area

$C$  = capacitor

$C_p$  = power coefficient

$E$  = back EMF

$L$  inductance

$p$  = number of pole pairs

$n_s/n_r$  = stator-to-rotor turns ratio

$P$  = active power

$Q$  = reactive power

$R$  = resistance

$S$  = apparent power

$T_e, T_s$  = electromechanical and shaft torque

$\beta$  = pitch angle

$\lambda$  = tip-speed ratio

$\rho$  = density of air or bandwidth of PLL

$\psi$  = flux modulus

$\omega_2$  = slip frequency

$\omega_r$  = (electrical) rotor speed of generator

PMG – Permanent Magnet Generator

IGBT - Insulated Gate Bipolar Transistor

PWM - Pulse Width Modulation

VSC - Voltage Source Converter



## CONTENTS

<b>Title Page</b> .....	i
<b>Abstract</b> .....	ii
<b>Acknowledgement</b> .....	iii
<b>List of figures</b> .....	iv
<b>List of tables</b> .....	v
<b>Nomenclature</b> .....	vi
<b>Chapter 1: Introduction</b>	
1.1 Introduction .....	1
1.2 Small Wind Turbines.....	2
1.3 Turbine Operating Parameters.....	4
1.4 The Power and Performance Curve.....	6
<b>Chapter 2: Literature Review</b>	
2.1 Components of Wind Electric Systems.....	11
2.2 Theoretical Analysis- Wind Turbine Model.....	12
2.3 Permanent Magnet Generator Model.....	13
2.4 Rectifier Model.....	14
2.5 Boost Chopper.....	15
2.6 PWM Inverter Model.....	16
<b>Chapter 3: Theoretical Development (Generator and Electrical System)</b>	
3.1 Introduction.....	18
3.2 Generators for Small Turbine.....	19
3.3 Rectifier, Inverter and Basic Control.....	23
<b>Chapter 4: Results and Discussion</b>	
4.1 Permanent Magnet Generator (PMG).....	27
4.2 Three-phase Uncontrolled Full-wave Rectifier.....	32
4.3 Step-up or Boost Chopper.....	34
4.4 PWM Inverter with Sine Wave Signal.....	36
4.5 Line Filters.....	39
<b>References</b> .....	41
<b>Appendix</b> .....	45

## **CHAPTER 1:**

# **INTRODUCTION**

## **1.1 INTRODUCTION**

Consumption of energy based on fossil fuel is considered to be the major factor for global warming and environment degradation. The utilization of naturally occurring renewable energy sources (RES) as an alternative energy supply has been assuming more importance of less power generation utilizing solar rays, geothermal energy, wind energy and wave energy has become a reality.

In the last years, a rising interest in non-contaminant energy source has emerged from the industrial and academic communities. Major RES, i.e. wind and solar are today economically feasible alternatives to conventional electric power generation. Among the various factors contributing to this success are the development of new technologies, new circuit topologies and novel control strategies.

Research on performance improvement of and cost reduction in such non-conventional energy conversion systems is being accorded the highest priority. Wind power generation has a strong connection to rotating machinery and hence its practical application is most promising. Wind generator control methods have been already proposed to efficiently utilize the wind power which is prone to fluctuation every moment. The induction type machine has the advantage of robustness, low cost and maintenance-free operation. However they have drawback of low power factor and need for an AC excitation source. Permanent magnet generator is chosen so as to eliminate the drawbacks of induction generator. Boost chopper circuit with a single switching device is choice for power control and provides an improved efficiency.

## 1.2 SMALL WIND TURBINES

- Small wind turbines are often located where the power is required or adjacent to the owner's home which may not be the windiest location, whereas wind farms containing large turbines are deliberately sited in windy areas.
- The generators of small turbines often have a significant resistive torque that must be overcome aerodynamically before the blades will start turning. Furthermore, pitch control is rarely used on small wind turbines because of cost. Thus it is not possible to adjust the blade's angle of attack to the prevailing wind conditions. This problem is particularly acute during starting.
- Small wind turbine aerodynamics is influenced strongly by low values of the Reynolds number,  $Re$ . Low values of  $Re$  mean, in practice, that small wind turbines bear greater similarity to model, rather than full-sized, aircraft, and hummingbirds rather than eagles.
- Large wind turbines have complex yaw drive mechanisms to align the rotor to the wind. These are usually deemed too expensive for small turbines, so some form of free yaw is used. The most popular options are to have a tail fin, like three of the five turbines shown in Fig.1.1, or to have downwind blades, as do the remaining two.
- Many small turbines rely on furling for overspeed protection whereas large turbines usually have a brake on the high speed shaft (after the gearbox and before the generator).

- The blades of all wind turbines are comprised of aerofoil sections whose purpose is to produce lift, which is the primary component of the torque about the turbine axis in the direction of blade rotation. For steady flow, the product of this torque and the blade angular velocity,  $\omega$ , gives the power extracted from the wind.

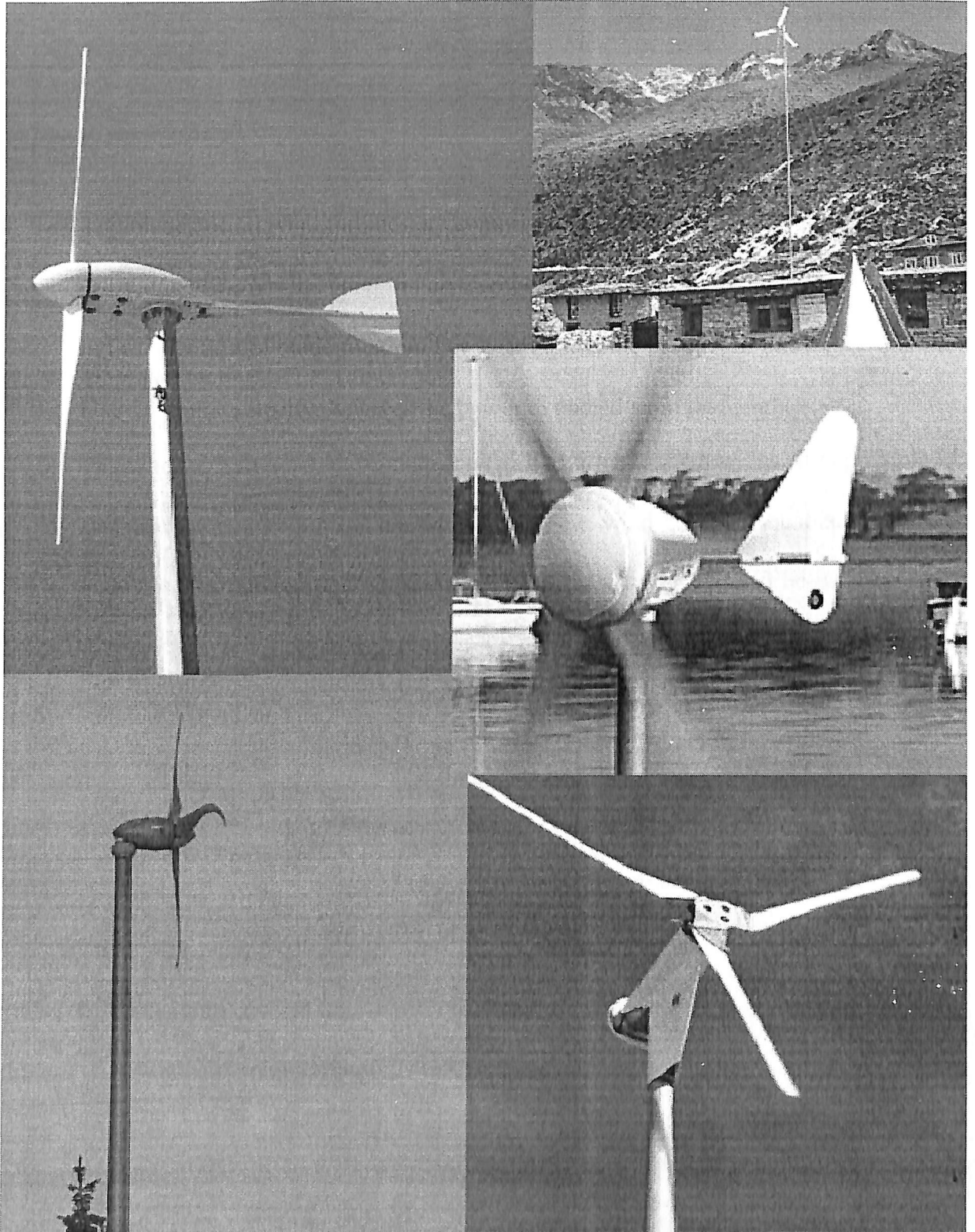


**Fig. 1.1** A range of small wind turbines.

### 1.3 TURBINE OPERATING PARAMETERS

As with any fluid machine, it is often useful to discuss wind turbine operation in terms of parameter groupings that can be obtained from dimensional analysis. Here the important parameters are introduced, the power coefficient,  $C_p$ , should be defined as

$$C_p = \frac{P}{\frac{1}{2}\rho U^3 \pi R^2}$$

$C_p$  the ratio of the actual power produced to the power in the wind that would otherwise pass the blade disk.

Note that:

- $C_p$  is dimensionless
- $C_p$  is not strictly efficiency, even though it is often treated as one. It is possible to increase  $C_p$  by increasing the velocity of the wind through the blades by, for example, surrounding the blades by a diffuser. However,  $C_p$  can be interpreted as efficiency when comparing turbines of the same type, such as the diffuser-less ones.

By making the very general statement that the turbine power should depend on wind speed, air density, turbine radius,  $X$ , and the kinematic viscosity of the air,  $\nu$ , then

$$f(P, U, \omega, \rho, R, \nu) = 0$$

where  $f$  denotes (the as yet unknown) functional dependence.  $\nu$  is the actual viscosity divided by the density, and has units of  $\text{m}^2/\text{s}$ . For sea level conditions,  $\nu = 1.5 \times 10^{-5} \text{ m}^2/\text{s}$  at  $20^\circ\text{C}$ .

Above equation contains six parameters or variables and three dimensions, so there should be three non-dimensional groups resulting from the dimensional analysis. To ensure that  $C_p$  is one of these groups, the “repeating variables” must be  $U_0$ ,  $q$ , and  $R$ . These repeating variables can, in principle, appear in all the non-dimensional groups. Forming these groups then allows to be rewritten as

$$f(C_p, \omega R/U, UR/v) = 0$$

The second of these groups is sufficiently important to have its own name, the tip speed ratio, and symbol  $\lambda$ .

$$\lambda = \omega R/U = V_{tip}/U$$

is the ratio of the circumferential velocity of the blade tips,  $V_{tip}$ , to the wind speed. In determining the lift and drag  $\lambda$  is critical as it sets the angle of attack of the blade sections or elements. Very simply: the tip speed ratio controls the blade aerodynamics. Usually,  $\lambda$  ranges from 7 to 10 for a turbine operating at maximum  $C_p$ . Thus the tips are travelling at a velocity that is many times the wind speed and this can cause them to approach the limit of incompressible flow, about 30% of the speed of sound, which is 340 m/s at typical sea level conditions. There is no evidence that compressibility is important on operating wind turbines.

The third group should be recognized as a Reynolds number,  $Re$ , which generally measures the importance of viscosity. The most useful form comes from considering the lift and drag behavior of the aerofoil sections that comprise the blades. This  $Re$  contains the blade chord,  $c$ —the width of the blade—and the “total” velocity at the blade,  $U_T$ , both of which vary along the blade. Thus

$$Re = U_T c / \nu$$

Most of a turbine's power is produced near the tip, so the value of  $Re$  most often quoted is the tip Reynolds number. If  $\lambda$  is sufficiently high,  $U_T \approx \lambda U$  at the tip, but  $U_T \approx U_0$  everywhere along a stationary or slowly rotating blade. For most large turbines, producing say 100 kW or more,  $C_P$  is not strongly dependent on  $Re$ , but, shows that  $C_P$  varies significantly with  $\lambda$ . Reynolds number effects can be significant for small turbines.

The final quantity of interest is the thrust on the blades,  $T$ . This force is not as important for wind turbines as it is for propellers, which are designed to produce thrust. However, the thrust is usually transmitted to the turbine tower, and so must be included in tower and foundation design. Dimensional analysis starts from the appropriately modified form of

$$f(P, U, \omega, \rho, R, v) = 0$$

from which the following form of the thrust coefficient,  $C_T$ , should be almost immediately recognisable as

$$C_T = \frac{T}{\frac{1}{2} \rho U^3 \pi R^2}$$

As with the power output,  $C_T$  is strongly dependent on  $\lambda$  but not usually on  $Re$ .

## 1.4 THE POWER CURVE AND THE PERFORMANCE CURVE

However much the aerodynamicist is happy to use non-dimensional groups to describe and analyse performance, the owner of the turbine is more interested in the actual power output as function of wind speed. This is given by the power curve. Figure 1.2 shows the power curve for the 7 m diameter Bergey BWC XL 10 kW turbine and Fig. 1.3 shows one for the 80 m diameter Vestas V80 2 MW turbine. Both sets of data are given in Table 1.1. Each figure indicates the "cut-in" wind speed below which no power is produced, approximately 3.5 m/s for both. Also important is the "rated" wind speed where the

advertised power is obtained; 13 m/s for the smaller machine and 15 m/s for the larger. It is common for the rated speed to increase with turbine size because the tower height also increases, and this increases the wind speed at the hub. Both turbines have a region, between 5 and 10 m/s, where the power increases rapidly, approximating the cubic dependence of wind speed. Because of the sensitivity of power to wind speed, it is important to take note of the rated speed; the easiest way for a manufacturer to “improve” the performance of a turbine is to increase the rated speed

After 10 m/s, the power output of both turbines increases less rapidly as the control system shifts away from attempting to maximise the power output. It is important to be able to control a turbine at high wind, so that it does not extract more power than can be absorbed by the generator. High power levels may also cause unacceptable structural loads on the blades and other components.

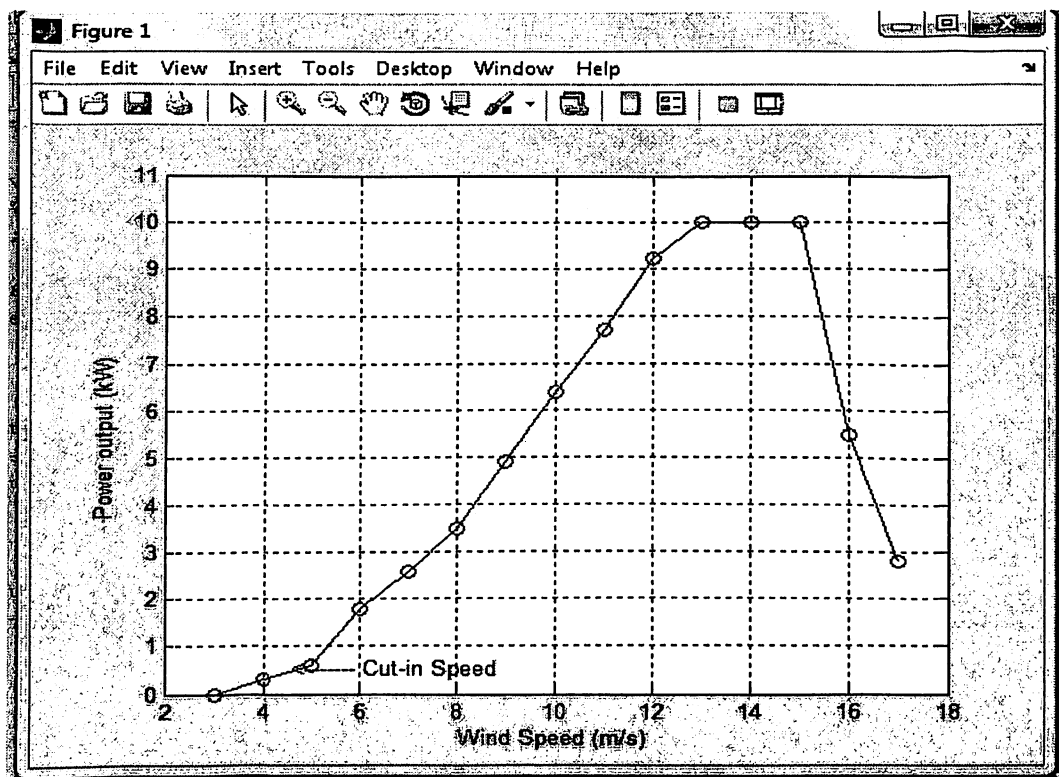


**Fig. 1.2 Power Curve for the 10 kW Bergy BWC Turbine at Sea Level. Data from**



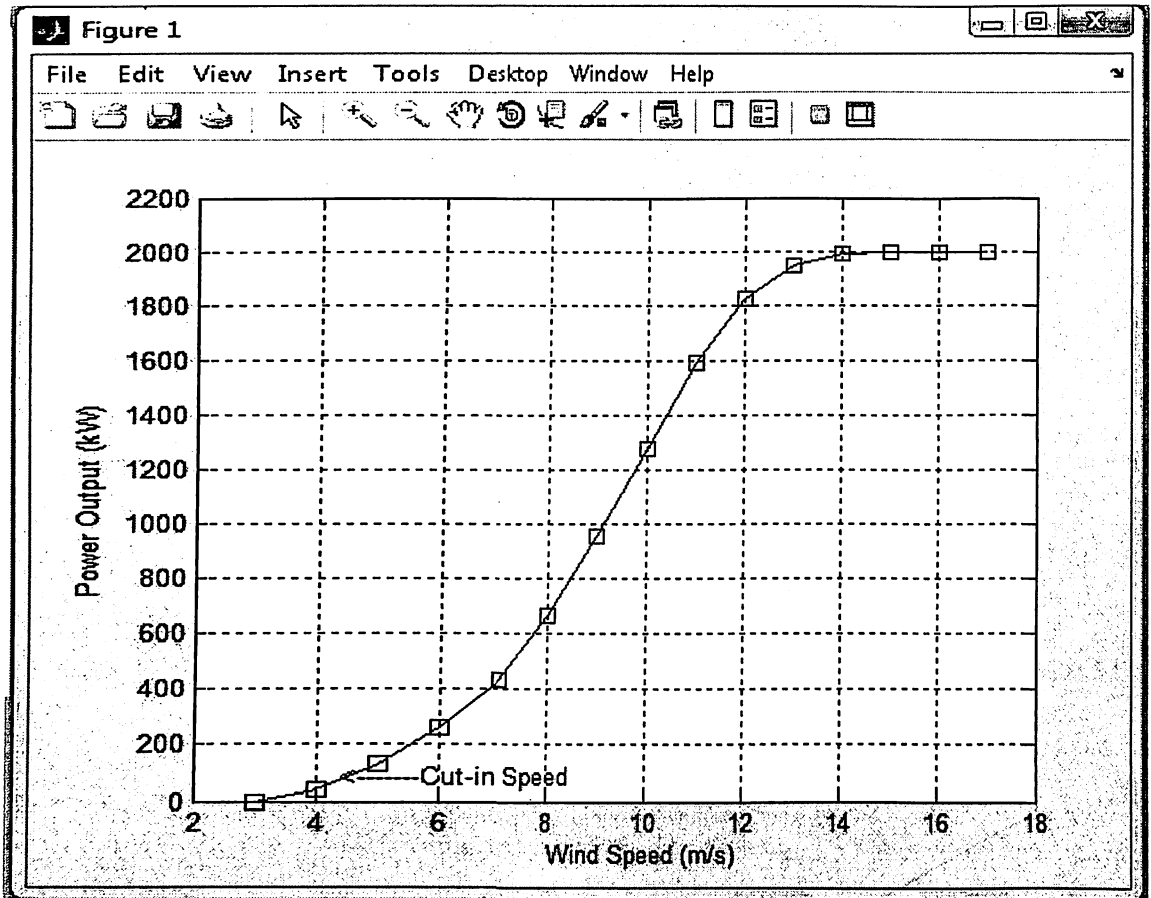


**Fig. 1.3 Power curve for the Vestas V80 turbine. Data from [www.restscreen.net](http://www.restscreen.net)**

There are a number of possible control actions for large wind turbines, such as controlling the angle of attack by pitching the blades, which are not available at small scale. For nearly all large turbines but rarely for small ones, there is also a “cut-out” wind speed at which the turbine is shut down for safety reasons. This is 25 m/s for the V80 (not shown in above Fig.). At this speed, the brake is activated, and not released until the wind has died down. At high wind speeds, smaller turbines such as the Bergey 10 kW, are often “furlled”, that is turned out of the wind direction by the collapse of the tail fin. Other small turbines rely on control of the generator’s field current to reduce output in high winds and shorting of the generator output for braking. This “electrical” rather than “mechanical” or “aerodynamic” braking.

Wind speed (m/s)	Vestas V80 2 MW		Bergey XL 10 kW	
	P (kW)	$C_p$	P (kW)	$C_p$
3	0	0	0	0
4	44.0	0.228	0.3	0.203
5	135.0	0.358	0.6	0.208
6	261.0	0.401	1.8	0.361
7	437.0	0.422	2.6	0.328
8	669.0	0.433	3.5	0.296
9	957.9	0.435	4.9	0.291
10	1279.0	0.424	6.4	0.277
11	1590.0	0.396	7.7	0.251
12	1823.0	0.350	9.2	0.231
13	1945.0	0.294	10.0	0.197
14	1988.0	0.240	10.0	0.158
15	2000.0	0.196	10.0	0.128
16	2000.0	0.162	5.5	0.058
17	2000.0	0.135	2.8	0.025

**Table.1.1 Power and power coefficient variation with wind speed for the Vestas V80 2 MW and Bergey XL 10 kW turbines**

As the wind speed increases from below the cut-in, the brake on larger turbines is released, and, the blades are pitched into the wind to assist in starting. In contrast, the lack of pitch adjustment on small turbines makes them rely on the lift generated at high angles of attack, to overcome the resistive torque of the drive train and generator.

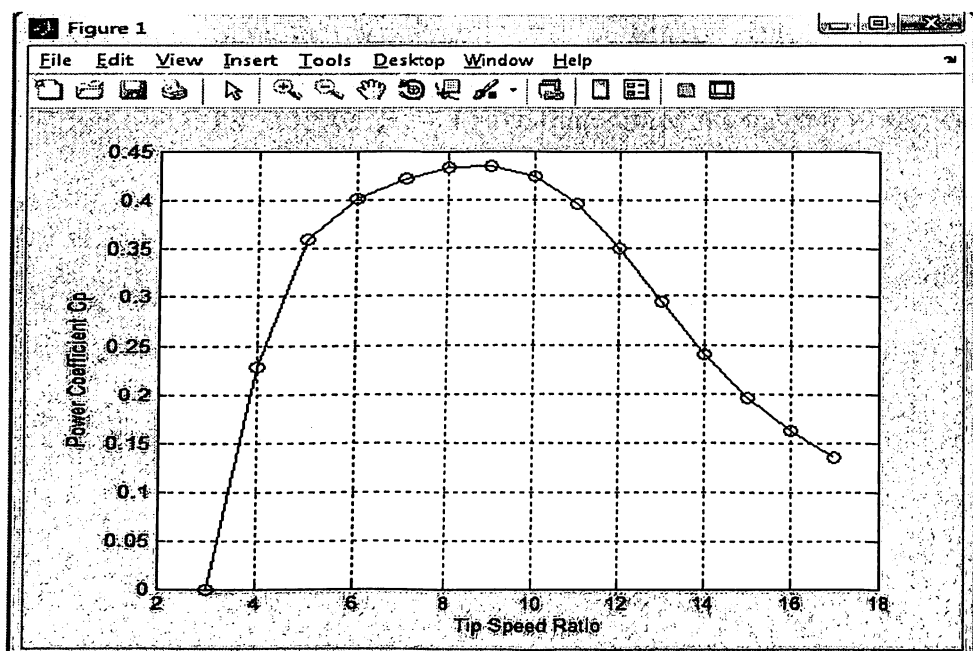


**Fig. 1.4 Power coefficient variation with tip speed ratio for the Vestas V80**

Figure shows that  $\lambda$  has a major effect on turbine performance. This is because it controls the angle of attack of the blades. Since the value of  $C_p$  determines how much power is extracted at a given wind speed, Fig. 1.4 implies that a constant speed turbine cannot operate at maximum efficiency over a large range of wind speed; obviously the turbine's designers have opted to forgo some of the extractable power for the simplicity of constant speed operation.

Figure 1.4 was generated from the power curve data by using the almost constant  $X$  of 16.9 rpm for the Vestas V80. The maximum  $C_p$  is nearly 0.44, but note that the power listed in Table 1.1 is the output electrical power which is less than the input aerodynamic power by the product of the efficiencies of the (mechanical) drivetrain and the (electrical) generator. Estimating the combined efficiencies as 0.9, indicates that the V47's maximum efficiency is within 20% of the Betz–Joukowski 2 limit of  $16/27 = 0.593$ , the supposed maximum efficiency of this type of turbine. It is unlikely that any turbine will be able to get significantly closer to the Betz–Joukowski limit. Figure 1.6 shows the general shape of any performance curve: as  $\lambda$  increases from zero,  $C_p$  increases to reach its maximum at the optimal value of  $\lambda$  and then decrease to zero at the “runaway” point where  $X$  is maximized. For the Vestas V80 the runaway  $k$  is probably around 20. Any turbine that loses its electrical load will accelerate towards runaway. The danger is that if the wind speed is high enough, the centrifugal forces within the blades will shatter them. Figure 1.6 shows why the current trend for both large and small turbines is to attempt to keep a constant  $\lambda$  as the wind speed varies. This is a major challenge for small turbines where the wind speed is not measured. The control strategy to achieve constant- $\lambda$  operation is an implementation of what is usually called “maximum power point tracking”, MPPT.

## CHAPTER 2:

# LITERATURE REVIEW

## 2.1 COMPONENTS OF WIND ELECTRIC SYSTEMS

The basic components of a wind electric system analyzed herein are shown in Fig 2.1. A step-up gear box and a suitable coupling connect the wind turbine to the Permanent Magnet Generator (PMG). The generated power of continuously varying frequency is fed to local load through suitable power converters, to ensure constant voltage and constant frequency. Since the wind power fluctuates with wind velocity, the generator output voltage and frequency vary continuously. The varying AC voltage is rectified into DC in a diode bridge and the dc voltage is then regulated to obtain constant voltage by controlling the duty ratio of a DC/DC boost converter. The DC voltage is inverted to get the desired AC voltage and frequency employing a PWM inverter. The duty ratio,  $\delta$  controls the boost chopper output voltage.

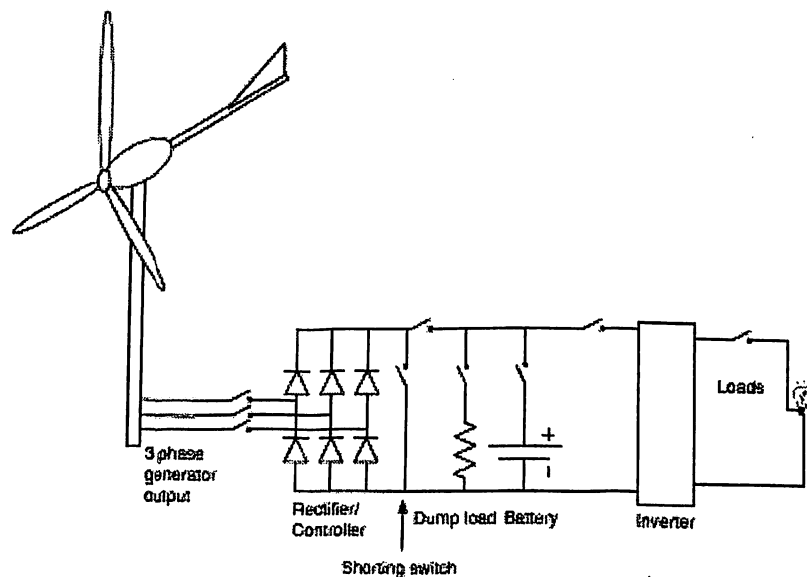


**Fig. 2.1: Small turbine system with basic circuit breaker and switch protection**

## 2.2 WIND TURBINE MODEL

There are two types of wind turbines namely vertical axis and horizontal axis types. Horizontal axis wind turbines are preferred due to the advantage of ease in design and lesser cost for higher power ratings.

The power captured by the wind turbines is obtained as

$$P = \frac{1}{2} \pi \rho R^3 V^2 C_p$$

Where the power coefficient  $C_p$  is a nonlinear function of wind velocity and blade pitch angle and is highly dependent on the constructive features and characteristics of the turbine. It is represented as a function of the tip speed ratio  $\lambda$  given by

$$\lambda = R\omega/V$$

It is important to note that the aerodynamic efficiency is maximum at the optimum tip speed ratio. The torque value obtained by dividing the turbine power by turbine speed is formed obtained as follows:

$$T_t (V, \omega) = \frac{1}{2} \pi \rho R^2 V^3 C_t(\lambda)$$

Where  $C_t(\lambda)$  is the torque coefficient of the turbine, given by

$$C_t(\lambda) = \frac{C_p(\lambda)}{\lambda}$$

The power coefficient  $C_p$  is given by

$$C_p(\lambda) = \left( \frac{1.16}{\lambda^1} - (0.4 * \beta) - 5 \right) 0.5 e^{-\frac{16.5}{\lambda^1}}$$

Where

$$\lambda_1 = \frac{1}{\left( \frac{1}{(\lambda + 0.089\beta)^4} + \frac{0.035}{\beta^3 + 1} \right)}$$

## 2.3 PERMANENT MAGNET GENERATOR MODEL

Permanent Magnet Generator provides an optimal solution for varying-speed wind turbines, of gearless or single-stage gear configuration. This eliminates the need for separate base frames, gearboxes, couplings, shaft draft lines, and pre-assembly of the nacelle. The output of the generator can be fed to the power grid directly. A high level of overall efficiency can be achieved, while keeping the mechanical structure of the turbine simple.

Generated emf/phase,

$$E = V_t + I_a (R_a + jX_s) = V_t + I_a Z_s$$

Where

$$Z_s = \sqrt{R_a^2 + X_s^2}$$

The rotor reference frames of the voltages are obtained as

$$V_q = -(R_s + L_q p) I_q - \omega_r L_d I_d + \omega_r \lambda_r$$

$$V_d = -(R_s + L_d p) I_d + \omega_r L_q I_q$$

The expression for the electromagnetic (EM) torque in the rotor is given by

$$T_e = \left(\frac{3}{2}\right) \left(\frac{Pn}{2}\right) [(L_d - L_q) I_q I_d - \lambda_m I_q]$$

The relationship between the angular frequency of the stator voltage ( $\omega_m$ ) is obtained as follows:

$$\omega_r = \frac{Pn}{2} \omega_m G$$

$$p\omega_r = \frac{Pn}{2Jg} (T_m - T_e)$$

$$p\theta = \omega r$$

Torque developed by the turbine  $T_t$  released to the input to the generator  $T_m$  is expressed as

$$T_m = \frac{T_t}{G}$$

## 2.4 RECTIFIER MODEL

A three phase diode bridge rectifier converts the AC generated output voltage, which will be varying in magnitude and also in frequency, into DC. The average output voltage of the three phase diode rectifier is obtained as follows:

$$V_{dc} = \frac{3V_m}{\pi}$$

And the average and RMS load currents are given by

$$I_{dc} = \frac{V_{dc}}{R_l}$$

$$I_{rms} = \frac{V_{rms}}{R_l}$$

## 2.5 BOOST CHOPPER

The conversion of rectified DC voltage to any specified DC output voltage can be carried out employing a DC-DC converter or chopper circuit.

The boost chopper output voltage is obtained as

$$V_o = V_s \frac{V_s}{(T - T_{on})}$$

$$V_o = \frac{V_s}{(1 - \delta)}$$

Where  $\delta$  = Duty ratio of the chopper

Table 2.1 shows the change of duty ratio chopper with respect to wind velocity. As the wind velocity changes the duty ratio of the chopper is adjusted in order to provide a constant output.

Table 2.1. Change of Duty Ratio of Chopper with respect to Wind Velocity

S. NO.	Wind Velocity in m/s	Duty Ratio
1	4	0.8618
2	5	0.8272
3	6	0.7926
4	7	0.7581
5	8	0.7235
6	9	0.689
7	10	0.6544



8	11	0.6198
9	12	0.8583
10	13	0.5507
11	14	0.5162
12	15	0.4816

## 2.6 PWM INVERTER MODEL

For providing electric power to industrial applications in the form of AC, the DC output of Boost Chopper is inverted in a three phase AC voltage. The most efficient of controlling the output voltage is to incorporate pulse width modulation control within the inverters. In this method, a fixed DC input voltage is supplied to the inverter and a controlled AC output voltage is obtained by adjusting the on and off periods of inverter devices. In the inverter output voltage of  $2\pi$  radians, each control signal has duration of  $\pi$  radians. The period  $T$  has been divided into six intervals. During each interval the switches receive control signals.

A switch conducts and carries current in the direction of its diode when the control signal is present and the switch is forward biased. The switch will always be forward biased, except when its anti parallel diode conducts and thus reverse biases the switch by its voltage drop. In any case, either the switch or its anti parallel diode will be in conduction during the presence of the control signal and the current will be flowed in either direction. During the interval I, the switch diode pairs  $S_{ap}$ ,  $S_{cp}$  and  $S_{bn}$  are in conduction. Hence, terminals A and C are connected to positive terminal of DC source and terminal B is connected to the negative terminal of the DC source.

Gating signal for PWM Inverter devices are generated employing a Sinusoidal Pulse Width Modulation Technique (SPWM), by comparing a sinusoidal reference signal with a triangular carrier wave. In this method of PWM, the harmonic content can be reduced using several pulse is varied proportional to the amplitude of a sine wave evaluated at the centre of the same pulse. The frequency of reference signals  $f_r$  determines the inverter output frequency  $f_0$  and its peak amplitude controls the modulation index  $M$  and this in turn the rms output voltage,  $V_0$ . The number of pulses per half cycle depends on the carrier frequency. By varying the modulation index, the rms output voltage can be varied.

If  $\delta_m$  is the width of the  $m^{\text{th}}$  pulse and  $p$  is the number of pulses, then the rms output voltage is obtained as:

$$V_{ac} = V_{in} \left( \sum_{m=1}^{2pul} \frac{\delta_m}{\pi} \right)^{\frac{1}{2}}$$

## CHAPTER 3:

# THEORETICAL DEVELOPMENT (Generator and Electrical System)

## 3.1 INTRODUCTION

Most early small turbines used DC generators. Modern practice favours three-phase AC permanent magnet generators (PMGs), with induction generators, often just a standard electric motor running “backwards”, as a fairly distant second choice. There are novel sources of PMGs, such as domestic washing machines, and an increasing number of them are being made especially for small wind turbines. Many of these come from China which has most of the world’s reserves of the rare earth magnetic materials needed for their manufacture.

This change of generators has been driven partly by consumer demand—there are many more AC-powered products than DC-powered—and partly by the advances in power electronics over the last 20 years or so. Nearly all modern generators are three-phase as this increases the ratio of power to weight and produces a more constant shaft torque in comparison to fewer phases. Even for grid connected small turbines, it is usual to rectify the varying frequency and voltage generator power and then invert it to produce AC power of constant voltage and frequency. This has become possible because of the significantly reduced cost and increased capability of modern inverters. Usually this conversion is combined with maximum power point tracking (MPPT) which aims to match the generator power output to the blade characteristics so as to extract the maximum possible power from the wind as its speed varies apparently randomly. MPPT is becoming standard on turbines above the micro category. Many micro-turbines charge batteries and use a much

simpler control system. Another more recent innovation is to combine the controller and inverter for grid connection.

Filtering is often used to reduce the harmonic distortion of the power supplied to the grid. The inverter must also control the power factor, and oversee the safe shutdown of the turbine if the grid is “lost”. In addition the turbine output must be synchronised with the grid. It is also becoming common for the turbine controller to have a major or exclusive role in over-speed protection. For example, the Skystream 2.4 kW turbine, uses shorting of the PMG output instead of aerodynamic controls such as furling and pitching. As with all forms of over-speed protection, there are potential problems with shorting the output. The current or heat generated may demagnetise the magnet and/or burn out the windings.

### 3.2 GENERATORS FOR SMALL TURBINES

Despite the demise of DC generators, it is worth mentioning them briefly. They are easy to control through the field current and small ones are cheap: even a portable electric drill or vacuum cleaner motor can be made to work as a DC generator. But they have brushes and a commutator, both of which wear out quickly. Since DC generators require a field current to provide the magnetic field, they have more losses than well designed PMGs, and are generally less efficient.

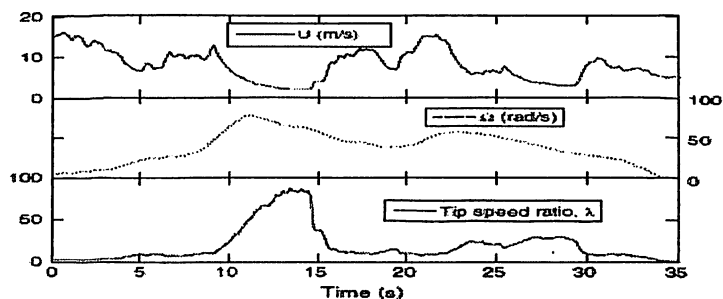


**Fig. 3.1 Over-speeding of the Aerogenesis 5 kW wind turbine**

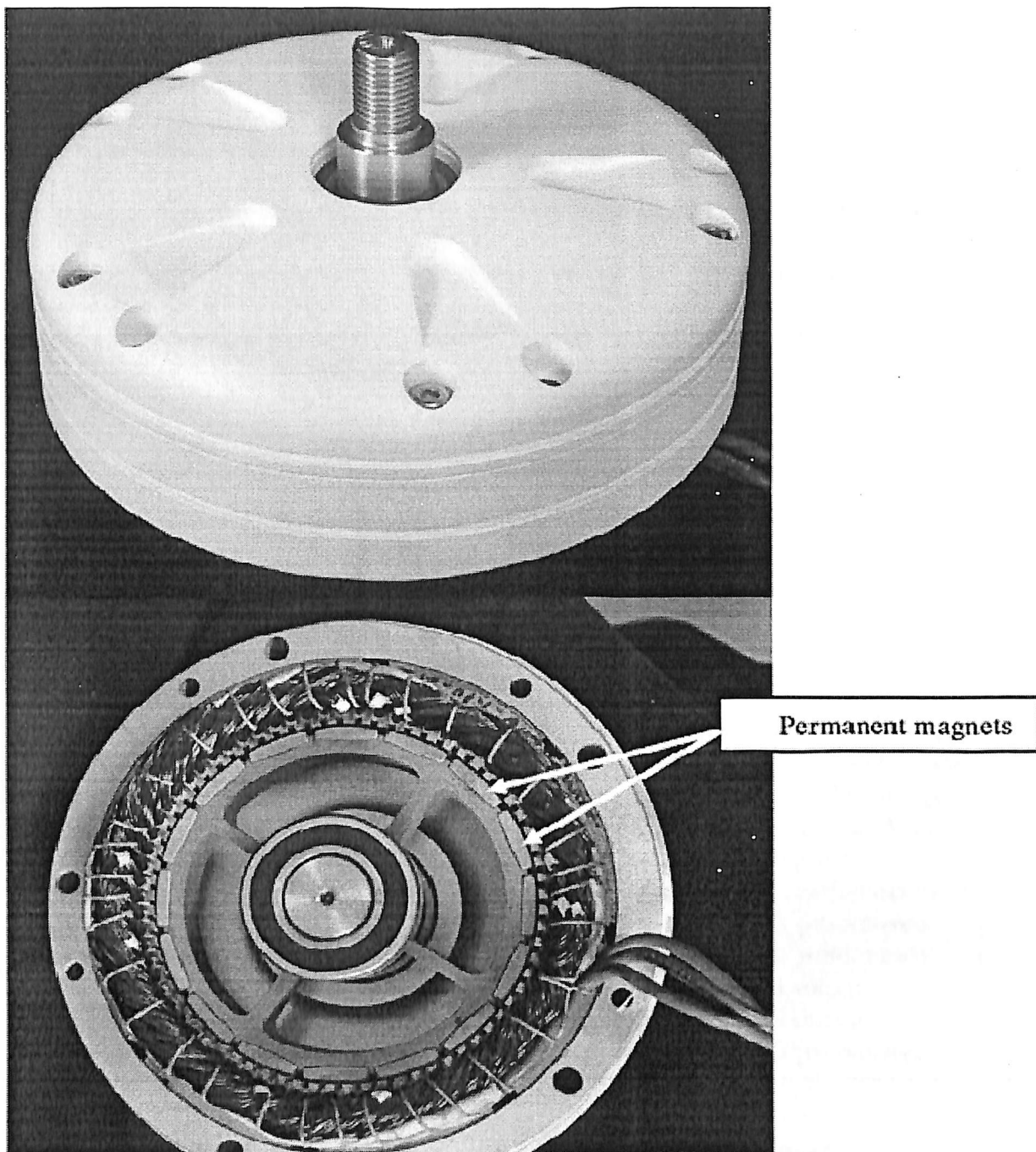


**Fig. 3.2 Outside and inside views of the Ginlong 500-A PMG. The casing outer diameter is 250 mm. The maximum shaft diameter is 34 mm. The 16 permanent magnets are attached to the rotor and the back bearing is clearly visible in the bottom photograph.**

Figure 3.2 shows the very simple structure of a PMG, in this case the Ginlong 500. The blade holder is normally bolted directly to the input shaft in Fig. 3.2. In addition to being

simple, PMGs with many poles—there are 16 poles on the PMG in Fig. 3.2—perform efficiently at low rpm which usually means they do not need a gearbox. The permanent magnets are attached to the rotor which rotates inside the stator carrying the windings. It can be appreciated that detachment of the magnets could cause major problems and be hard to repair. At least some rare earth magnets (e.g. NeFeB) can burn if the protective coating is worn off by striking part of the stator. Some PMG rotors have a lining of fibreglass or iron to keep the magnets in place. All PMGs should have a maximum speed rating below which it is guaranteed to keep the magnets in place for the lifetime of the generator.

Parameter	Value	Comments
Rated shaft input power	510 W	For blade design
Rated rotor speed	450 rpm	For blade design
Rated input torque	14.8 Nm	For blade design
Cogging torque	0.5 Nm	For blade design
Generator inertia	0.006 kg m <sup>2</sup>	Negligible in comparison to blade inertia
Generator weight	12.7 kg	For turbine platform and tower design
Rated stator phase voltage	20 V	ms line to line for rectifier design
Rated stator current	14.4 A	ms line to line for rectifier design
Number of poles	16	Determines operating rpm
Stator resistance	0.35 Ohm	For modeling PMG performance
d-Axis synchronous reactance $L_d$	3.305 mH	For modeling PMG performance
q-Axis synchronous reactance $L_q$	3.305 mH	For modeling PMG performance
DC bus voltage at rated speed	25 V	Maximum rectified voltage
DC bus current at rated output	20 A	Maximum rectified current
Permanent magnet flux density $\lambda_{pm}$	0.36 V/(rad/s)	For modeling PMG performance

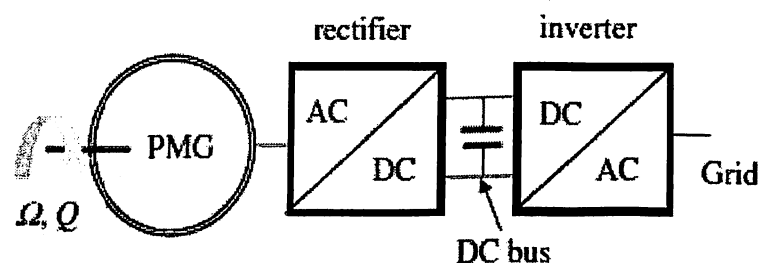
**Table 3.1 Main parameters of the Ginlong 500-A PMG**

Table 3.1 indicates their use in turbine design, modeling, and/or converter design. The maximum efficiency of the generator normally occurs at its highest voltage (which means rated speed, or higher), because for the same power output, the generator current is less. Conduction or “copper” losses increase with an increase in the generator current as the wires get hotter. There are losses from the generator iron being magnetised and

demagnetised many times per rotation (called iron losses). These losses depend on the magnetic field strength and the generator speed.

A PMG operated at a constant rpm produces maximum power when the load impedance matches that of the generator. This can be achieved by adding capacitance, but the amount needed is dependent on generator speed (i.e. frequency) and maximum power transfer comes at the price of a dramatic loss in efficiency. For a wind turbine, which must operate efficiently over a wide range of loads and frequencies, better load matching is needed. For the rectifier/controller–inverter topology shown in Fig. 3.3 matching can be achieved through pulse-width modulation (PWM).

The PMG produces three-phase power of varying voltage and frequency which is normally rectified to DC. If the turbine is charging batteries then they would replace the inverter in the schematic. This possibility may have been in the mind of the designer of the Ginlong 500-A PMG as the DC bus voltage slightly higher than 24 V which is one of the common voltages used in battery banks for remote power systems.



**Fig. 3.3 Schematic of a PMG wind turbine feeding the grid. The filtering of the inverter output and possible isolation transformer are not shown**

Table 3.1 shows that the cogging torque is small compared to the rated torque even though the ratio is relatively high for this PMG. The smallness of the cogging torque means that it is only important for starting and low speeds. Furthermore, it is possible to design the

control system to counteract it. Cogging torque is easy to measure. In practice, cogging torque can be reduced significantly, but it is very difficult to eliminate without using iron-less generator designs.

### 3.3 RECTIFIERS, INVERTERS, and BASIC CONTROL

This is the area of greatest and continuing advance in turbines of all sizes. One of the simplest power converters is the diode rectifier as diodes turn on and off naturally without the need for any control electronics. A 3-phase diode rectifier is shown in Fig. , where A, B, and C represent the three phases of the generated AC. The diodes have been numbered 1–6 in the standard manner corresponding to the order in which the diodes turn on. Normally, two diodes are on at the same time; one diode in the top half of the rectifier providing output current,

and one diode in the bottom half of the rectifier providing a return path for the DC bus current (i.e. if diodes 1 and 2 are on, this is followed by diodes 2 and 3 on, followed by diodes 3 and 4 on, and so forth).

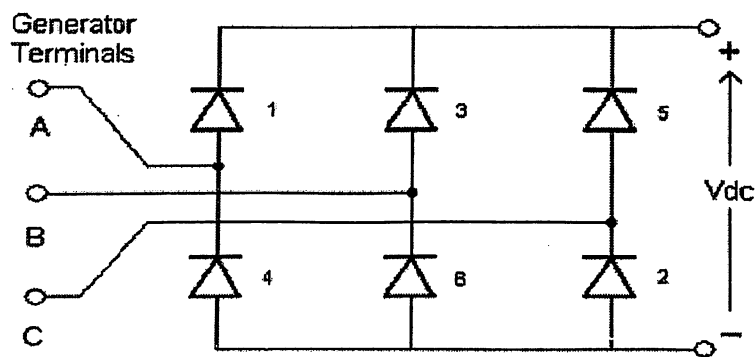


**Fig. 3.4 Schematic of a 3-phase diode rectifier**

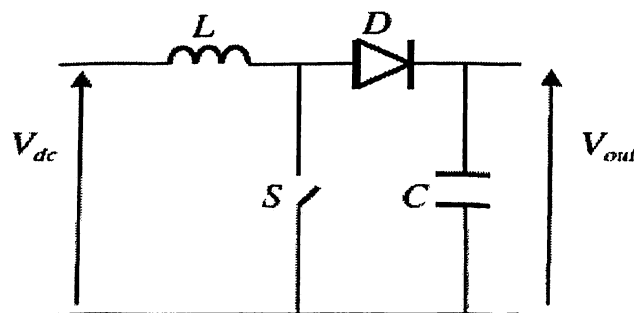


Figure 3.5 shows a simple boost converter where the input voltage  $V_{in}$  comes from the rectifier and the output voltage  $V_{out}$  is the DC bus voltage.  $L$ ,  $D$ , and  $C$  are the inductance, diode, and capacitor, respectively, and  $S$  is the

IGBT whose switching can be controlled to provide PWM.  $V_{out}$  is related to  $V_{in}$  by the remarkable equation

$$V_{out} = V_c / (1 - a)$$

which is independent of  $L$ ,  $D$ , and  $C$  whose values are fixed by the need to maintain “continuous conduction” and keep within the maximum allowable AC ripple in  $V_{out}$ .  $a$  is the duty cycle, the fraction of time that the switch is shut.  $V_{out}$  is greater than  $V_{dc}$  and greater than the peak AC voltage from the inverter if one follows the boost converter. However, if  $V_{out}$  is too large with respect to  $V_{dc}$  then  $a$  must be made large and diode  $D$  must transfer a lot of energy to the capacitor  $C$  in a short period of time. This stress on the diode and capacitor reduces boost converter efficiency: the maximum practical boost factor  $1/(1 - a)$  is about 3. Note on the other hand that if  $V_{out}$  is too close to  $V_{dc}$  then  $a$  must be made small with the consequence that switch  $S$  must quickly transfer significant energy to the inductor  $L$  which may again reduce boost converter efficiency. A buck-boost converter, having the ability to step-up or step-down the DC bus voltage, may be used in place of the boost converter to overcome switching stresses.



**Fig. 3.5 Schematic of a simple IGBT boost converter**

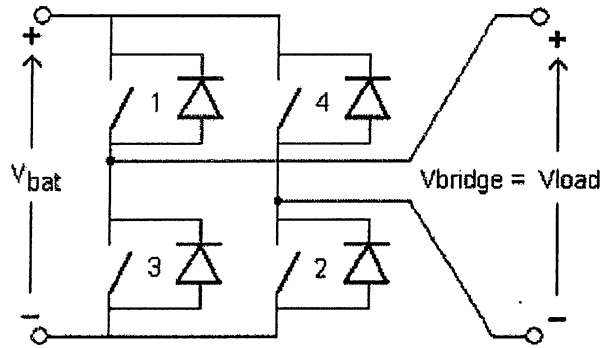


**Fig. 3.6 A simple single phase full-bridge inverter**

AC output power requires an inverter to convert the DC voltage into a fixed frequency and voltage waveform. A simple single phase “bridge” inverter is shown in Fig. 3.6 where  $V_{bat}$  is either the DC voltage from the battery bank or  $V_{out}$  from the boost converter in Fig. 3.5. The term “bridge” refers to the output of the inverter which “bridges” the “legs” of the inverter (devices 1 and 3 form one leg while devices 2 and 4 form the second leg of the inverter). No filter is employed, thus the load voltage waveform,  $V_{load}$ , is not sinusoidal, Fig 3.7.

Nonetheless, this approach is sometimes taken to make cheap inverters for lowpower applications.

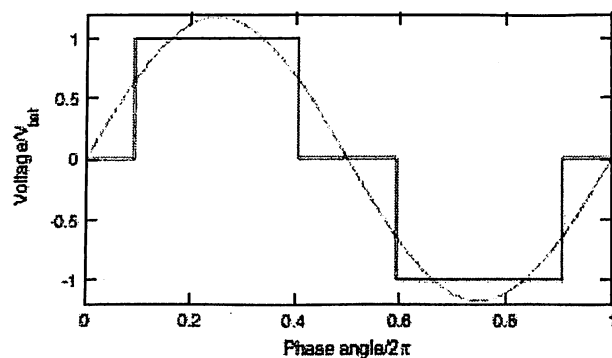


**Fig. 3.7 Modified square wave load voltage waveform for a single-phase inverter without a filter**

Most electrical devices, such as computers, home appliances, and motors (with a slight derating), can work well on modified-square-wave quality AC, but some require very close-to-sinusoidal power. Audio equipment, for example, will often produce a noticeable hum when powered by poor quality AC. To obtain a better approximation to a sinusoidal load voltage waveform a filter could be added and/or a more sophisticated PWM gating algorithm employed to control the timing of the IGBT switching devices. The four switching devices in Fig. 3.6 (or six devices in the case of a 3-phase inverter) can be manufactured individually with or without the feedback diodes; alternatively, the entire set of IGBTs with feedback diodes can be manufactured in a single module.

## CHAPTER 4:

# SIMULATION, RESULTS AND DISCUSSION

## 4.1 PERMANENT MAGNET GENERATOR (PMG)

The Permanent Magnet Synchronous Machine block operates in either generator or motor mode. The mode of operation is dictated by the sign of the mechanical torque (positive for motor mode, negative for generator mode). The electrical and mechanical parts of the machine are each represented by a second-order state-space model. The sinusoidal model assumes that the flux established by the permanent magnets in the stator is sinusoidal, which implies that the electromotive forces are sinusoidal. For the trapezoidal machine, the model assumes that the winding distribution and flux established by the permanent magnets produce three trapezoidal back EMF waveforms.

Mathematical Models for PMG:

Sinusoidal Model Electrical System

These equations are expressed in the rotor reference frame (qd frame).

$$\frac{d}{dt}i_d = \frac{1}{L_d}v_d - \frac{R}{L_d}i_d + \frac{L_q}{L_d}p\omega_r i_q$$

$$\frac{d}{dt}i_q = \frac{1}{L_q}v_q - \frac{R}{L_q}i_q - \frac{L_d}{L_q}p\omega_r i_d - \frac{\lambda p\omega_r}{L_q}$$

$$T_e = 1.5 p[\lambda i_q + (L_d - L_q)i_d i_q]$$

Where (all quantities in the rotor reference frame are referred to the stator)

$L_q, L_d$  .....q and d axis inductances

$R$  .....Resistance of the stator windings

$i_q, i_d$  .....q and d axis currents

$v_q, v_d$  .....q and d axis voltages

$\omega_r$  .....Angular velocity of the rotor

$\lambda$  .....Amplitude of the flux induced by the permanent magnets of the rotor in the stator phases

$p$  .....Number of pole pairs

$T_e$  .....Electromagnetic torque

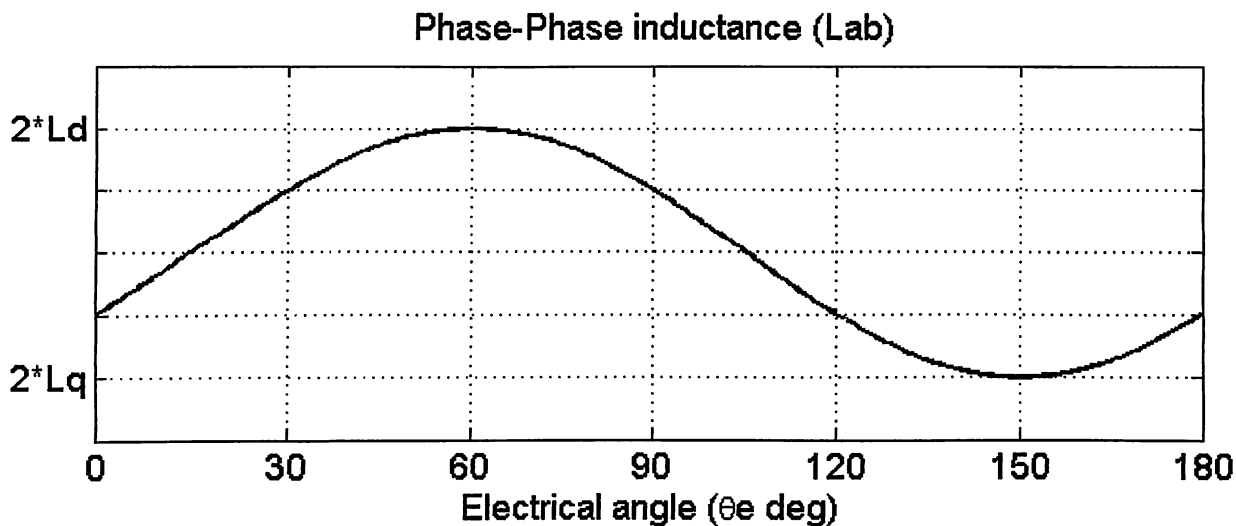
The  $L_q$  and  $L_d$  inductances represent the relation between the phase inductance and the rotor

position due to the saliency of the rotor. For example, the inductance measured between phase

a and b (phase c is left open) is given by:

$$L_{ab} = L_d + L_q + (L_q - L_d)\cos\left(2\theta_e + \frac{\pi}{3}\right)$$

Where  $\theta_e$  represents the electrical angle.



- For a round rotor, there is no variation in the phase inductance. Therefore,

$$L_d = L_q = L_{ab}/2$$

- For a salient round rotor, the dq inductances are given by:

$$L_d = \max(L_{ab})/2$$

And

$$L_q = \min(L_{ab})/2$$

### Trapezoidal Model Electrical System

These equations are expressed in the phase reference frame (abc frame). Note that the phase inductance  $L_s$  is assumed constant and does not vary with the rotor position.

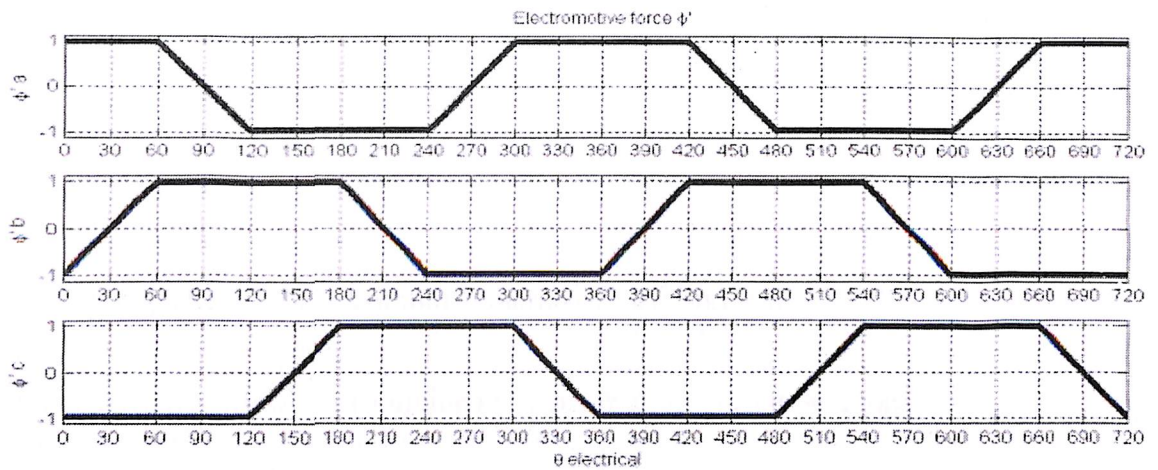
$$\frac{d}{dt}i_a = \frac{1}{3L_s}[2v_{ab} + v_{bc} - 3R_s i_a + \lambda p \omega_r (-2\Phi'_a + \Phi'_b + \Phi'_c)]$$

$$\frac{d}{dt}i_b = \frac{1}{3L_s}[-v_{ab} + v_{bc} - 3R_s i_b + \lambda p \omega_r (\Phi'_a - 2\Phi'_b + \Phi'_c)]$$

$$\frac{d}{dt}i_c = -\left(\frac{d}{dt}i_a + \frac{d}{dt}i_b\right)$$

$$T_e = p\lambda(\Phi'_a \cdot i_a + \Phi'_b \cdot i_b + \Phi'_c \cdot i_c)$$

where the electromotive force  $\phi$  is represented by



And

$L_s$  .....Inductance of the stator windings

$R$  .....Resistance of the stator windings

$i_a, i_b, i_c$  .....a, b and c phase currents

$\phi_a', \phi_b', \phi_c'$  .....a, b and c phase electromotive forces

$V_{ab}, V_{bc}$  .....ab and bc phase to phase voltages

$\omega_r$  .....Angular velocity of the rotor

$\lambda$  .....Amplitude of the flux induced by the permanent magnets of the rotor in the stator phases

$p$  .....Number of pole pairs

$T_e$  .....Electromagnetic torque

Mechanical System (for both models)

$$\frac{d}{dt} \omega r = \frac{1}{J} (T_e - F\omega r - T_m)$$

$$\frac{d\theta}{dt} = \omega r$$

Where,

J .....Combined inertia of rotor and load

F .....Combined viscous friction of rotor and load

T .....Rotor angular position

T<sub>m</sub> .....Shaft mechanical torque

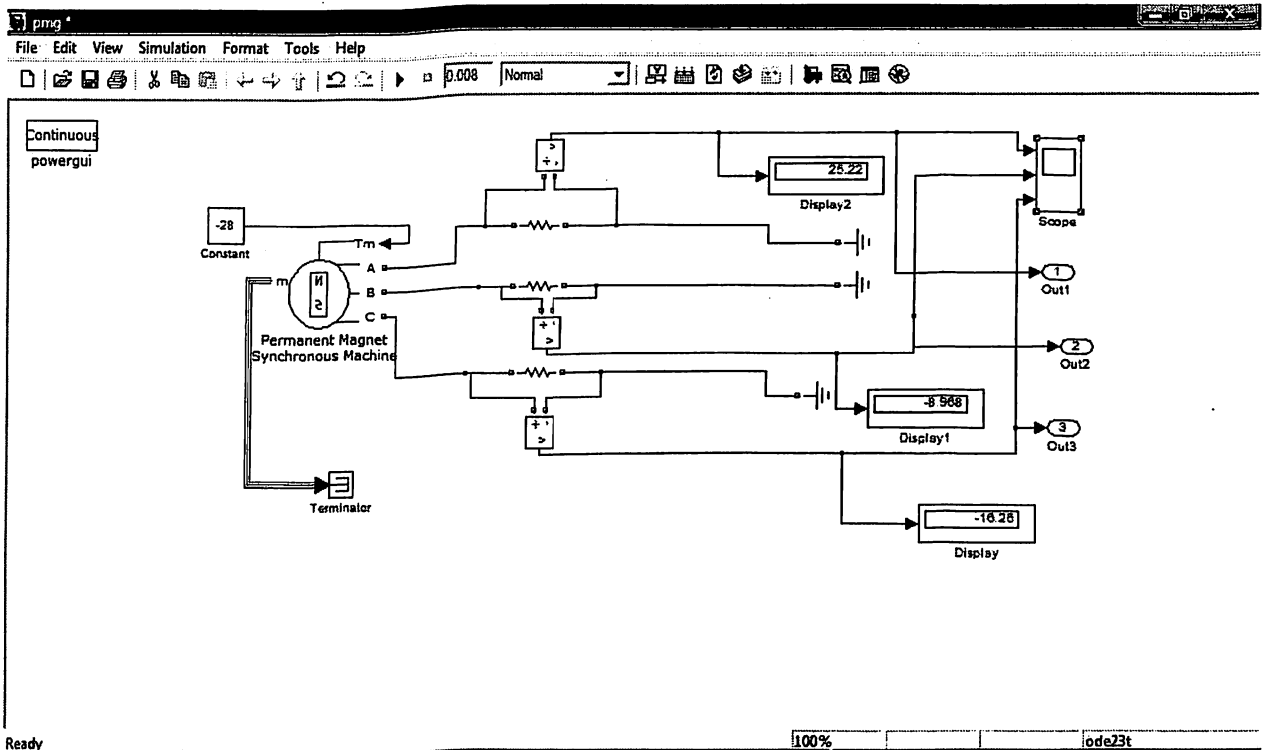


Fig. 4.1 Permanent Magnet Generator



## Results:



**Fig. 4.2** Waveforms of output voltages of permanent magnet generator

## 4.2 THREE-PHASE FULL-WAVE RECTIFIER

The functions of a three-phase full-wave rectifier are similar to that of a single-phase full-wave rectifier except that the input signal is three phase and six diodes are used for rectification.

The three-phase rectifier can be used for converting a three-phase AC supply into a DC or high voltage DC supply. A bridge-type three-phase full-wave rectifier model is shown in Fig. It contains six diodes D1, D2, D3, D4, D5, and D6. Diodes D1, D3, and D5 are ON when phase voltages V1, V2, and V3 are positive. Similarly, diodes D2, D6, and D4 are ON when phase voltages V1, V2, and V3 are negative.

For the continuous supply of current to the load, it is necessary that any one pair of diodes is ON at any instant of time during each input cycle. For instance pulse V1 is most positive

and V3 is most negative, then diodes D1 and D2 are ON and the load current flows from A to B. similarly, when phase V2 is most positive and V3 is most negative, diode D3 and D2 are ON. In the model shown in Fig. 4.3, the supply voltage the supply voltage is 315 V, 50 Hz, three-phase and the load resistance is of 105  $\Omega$ . The voltage across diode D1 and D2 is shown in Fig. Load current and voltage waveforms are shown in Fig. It can be observed that the load voltage is in phase with the load current and the output ripple frequency is 300 Hz. So, each diode conducts for the period of  $2\pi/6$  in one output cycle. The following measurements are taken for the model:

$V_{avg}$  and  $V_{rms}$  can be evaluated as follows:

$$V_{avg} = \frac{6}{\pi} \int_0^{\pi/6} 15 \sin(\omega t) d(\omega t)$$

$$= 24.44 \text{ V}$$

$$V_{rms} = \left[ \frac{6}{\pi} \int_0^{\pi/6} \{15 \sin(\omega t)\}^2 d(\omega t) \right]^{0.5}$$

$$= 24.44 \text{ V}$$

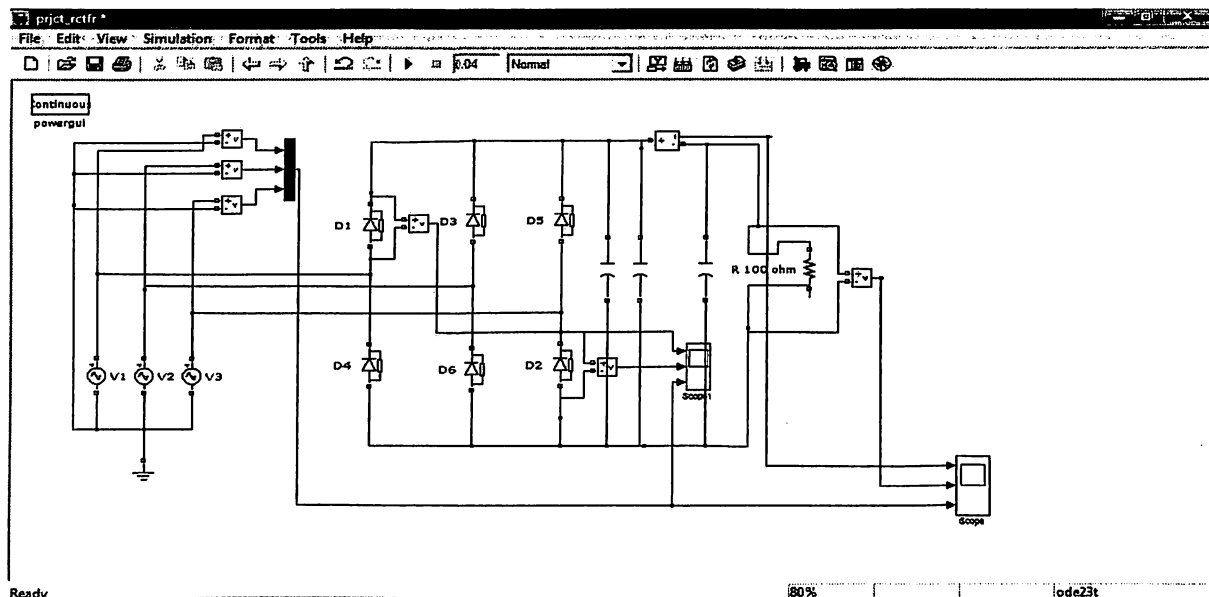


**Fig. 4.3 Three-phase full-wave rectifier**

**Results:**

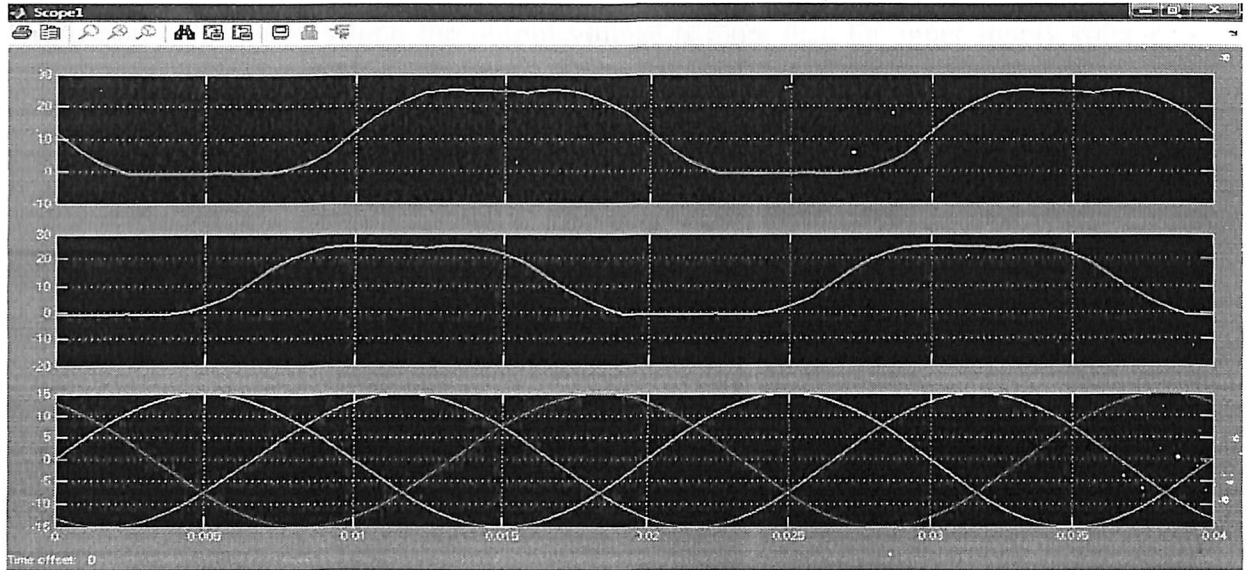


**Fig. 4.4 Voltage waveform across diodes D1 and D2 and input supply**

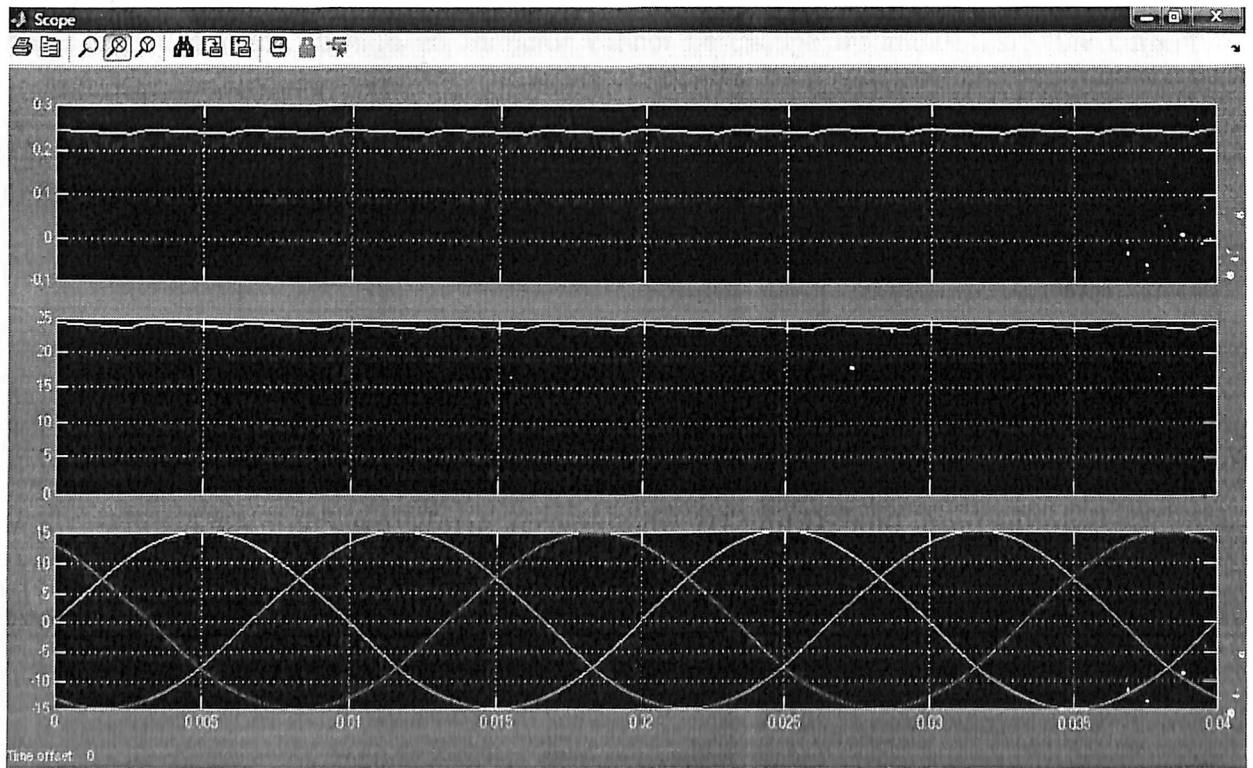


**Fig. 4.5 Current and voltage waveform for the resistive load**

### 4.3 STEP-UP OR BOOST CHOPPER

The chopper circuit in which the output voltage is more than the input supply voltage is called step-up chopper or boost chopper. A step-up chopper or boost converter model containing a 10V DC source, pulse generator, inductor of 5 mH, MOSFET switch, diode, capacitance of 90 $\mu$ F connected across the load resistance of 21.5 $\Omega$ , and measuring instruments is shown in fig. 4.6 The parameters set for the gate pulse block are as follows: Amplitude - 5, period - 0.01 s, pulse width - 50%, and phase delay - 0 s. In this circuit model, an inductance of 5 mH is connected in series with the voltage source through inductor and switch S1. This current charges the inductor and it stores energy. Now, when S1 is turned OFF, the current path changes and it starts flowing through the diode to the load. As the current through an inductor cannot be change instantaneously, the current decreases gradually through the load resistance. As the current tends to decrease, polarity of the EMF induced in the conductor is reversed and it adds up to the source voltage. Thus, the output voltage increases, i.e.  $V_{out} = V_s + L(di/dt)$ .

In this manner, this chopper acts as a step-up chopper and the energy stored in the inductor is released to the load. Figure 4.7 shows the inductor current, load voltage, and current waveforms obtained after simulating the circuit. The average output voltage measured was 19.94 V. The average output voltage of this chopper is given as follows:

$$V_{out} = (T/T_{off}) \times V_s = (T/(T - T_{out})) \times V_s = \{1/(1 - D)\} \times V_s$$

Therefore the duty cycle of 50%,  $V_{out}$  for this circuit will be  $10/0.5 = 20$  V ( $V_s = 10$  V). As duty cycle of the switch cannot be greater than 1, the output voltage is always greater than the input voltage. The output voltage can be varied by changing the duty cycle or  $T_{on}$  of the switch.

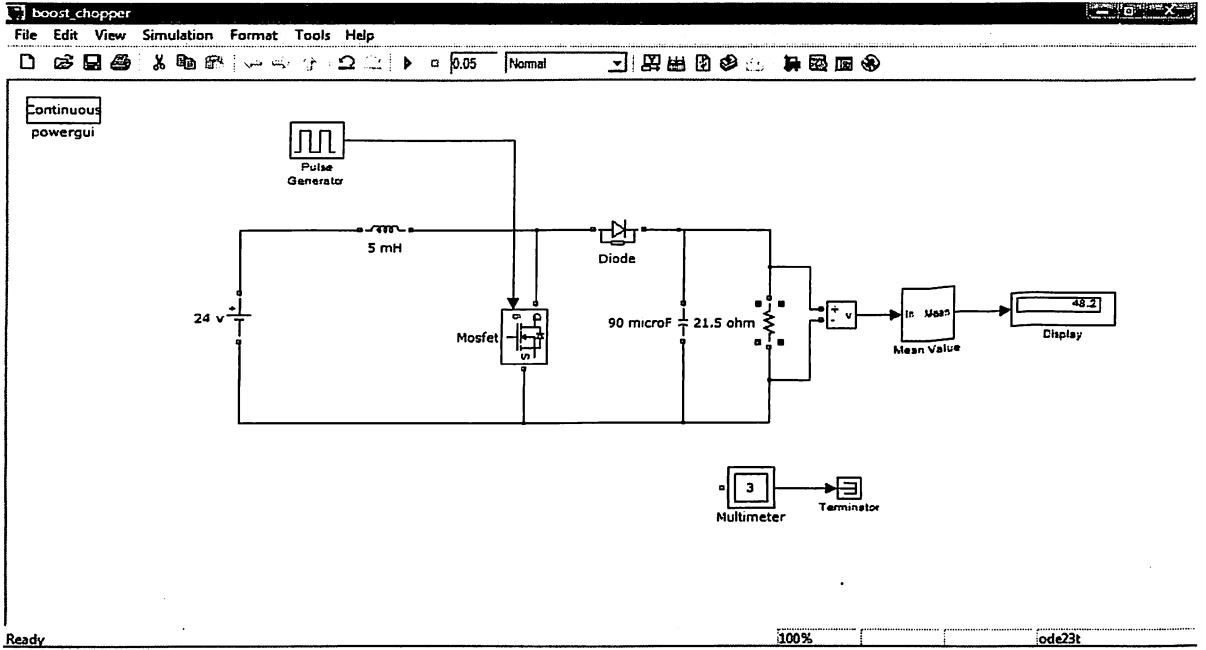


Fig. 4.6 Boost Chopper

Results :

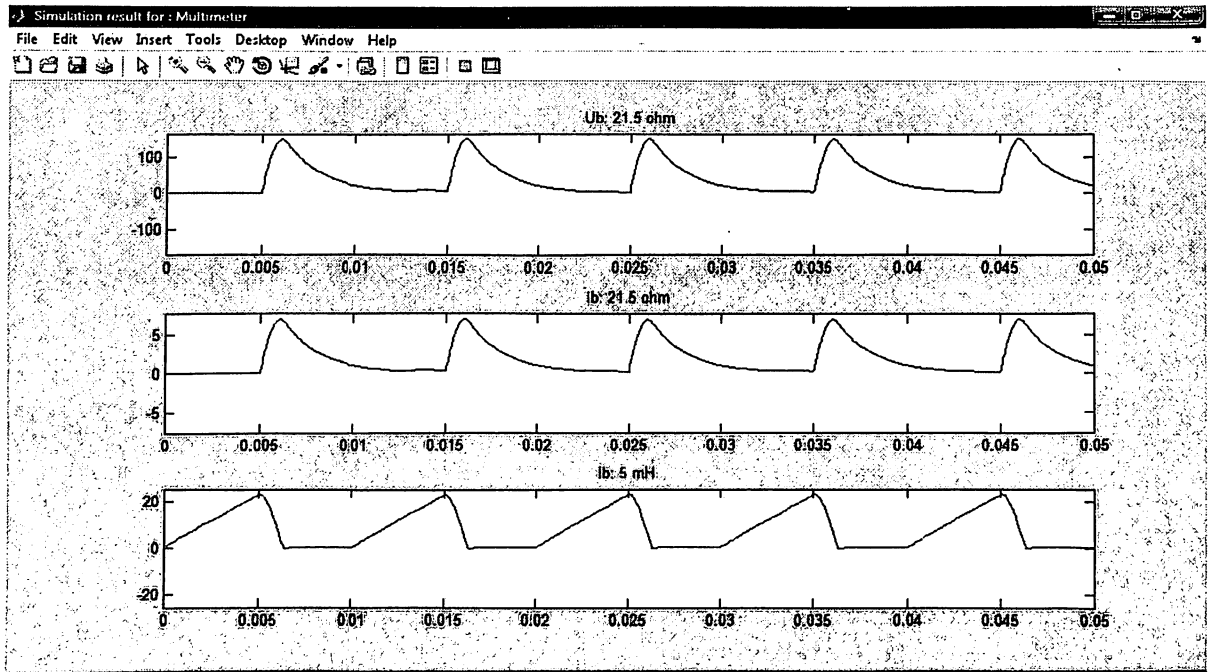


Fig. 4.7 Waveforms of the load voltage, load current, and current through the inductor

## 4.4 PWM INVERTER

In most of the inverter industrial application, the magnitude of the output voltage and the input of the DC voltage varies continuously, This requires continuous variation of the control pulse width in order to achieve the desire output voltage waveform. In this method, a reference signal is compare with high frequency triangular wave to generate PWM signal, If the reference signal is sin wave, the modulation is called sin wave pulse width modulation (SPWM).

The SPWM is realized by comparing a sin wave reference signal ( $V_r$ ) with high frequency triangular or swatooth wave signal ( $V_c$ ). The ratio of  $V_r/V_c$  is called modulation index (MI), and it determine the harmonic contain in the inverter output voltage. The frequency of the reference determines the output voltage frequency. And it peak magnitude determine the modulation index, which is turn determines the RMS output voltage. When the reference signal is compare with the carrier signal, their intersection is determine the switching instants of the inverter switches. When the magnitude of the reference signal is greater than the carrier signal the output of the comparator is high, otherwise the output is low. the output of the comparator is further processed such that the output pulse width of the inverter is same as that comparator . The circuit model of the PWM is shown below. This consist of sin wave block, Signal generator, switches, Constant block constant block, sum block, gain block and a scope. The sine wave signal is of amplitude 10 and frequency of 314 rad/sec. The carrier wave is saw-toothed signal of amplitude 10 and frequency 1KHz. The carrier signal is subtract from the reference signal for their comparison, The output is obtained is a PWM signal of varying magnitude. This signal is fed to input2 of the switch block. Input1 of the switch block is connected with a constant value of 5 and Input3 of the switch is connect to the constant value 0.. the selection criteria is taken as

$u_2 \geq$  threshold values is zero, the output of the switch is 5, otherwise zero. for three phase system we have to take three different PWM inverter signal, where we change the phase difference of 120 degree.

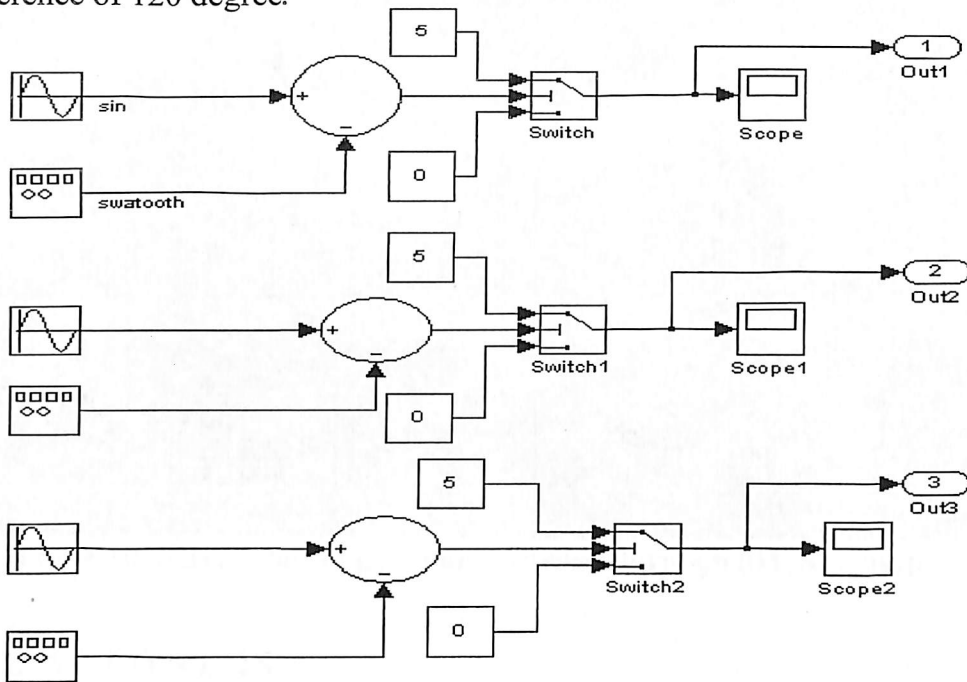
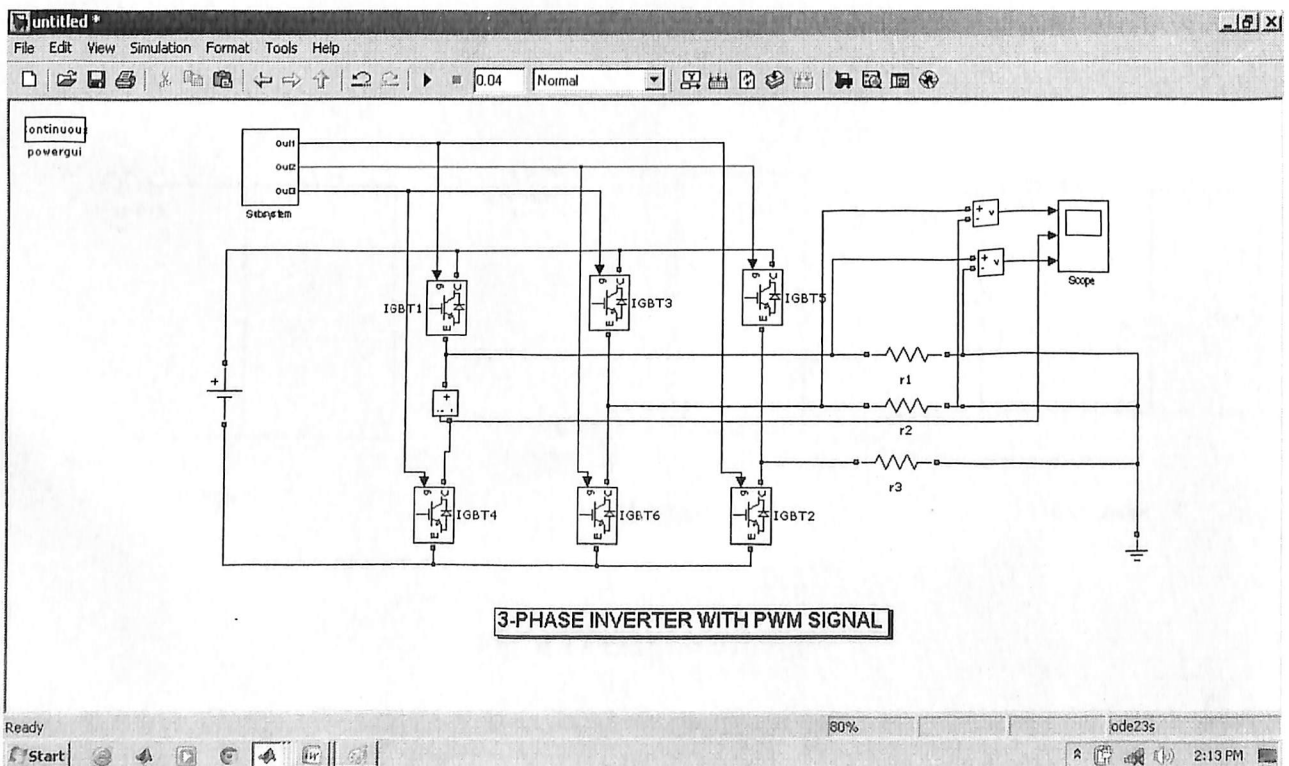


**Fig. 4.8 PWM pulse generator**

A block diagram of three phase PWM generator is shown below. The inverter consists of IGBT switches connect to the DC supply. When signal one is high then switches IGBT1 and IGBT2 is connected, when signal2 is high than IGBT5 and IGBT6 is connected, otherwise IGBT3 and IGBT4 is connected.



## Results:

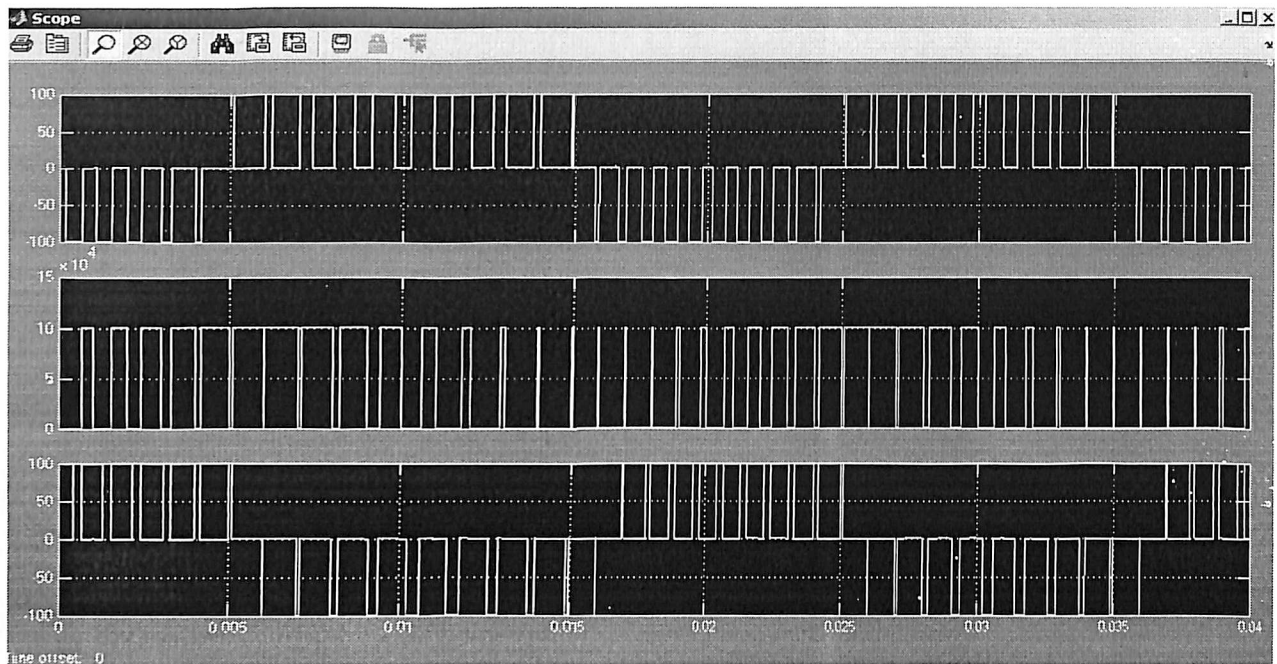


Fig. 4.10 Waveforms of gate pulse, current through M1, and output voltage

## 4.5 LINE FILTERS

To reduce the output harmonics, output filters are necessary. Fig. shows the commonly used output filters. A C filter is very simple, but it draws more reactive power. An LC-tuned filter as in Fig. can eliminate only one frequency. A properly designed CLC filter as in Fig. is more effective in reducing harmonics of wide bandwidth and draws less reactive power.

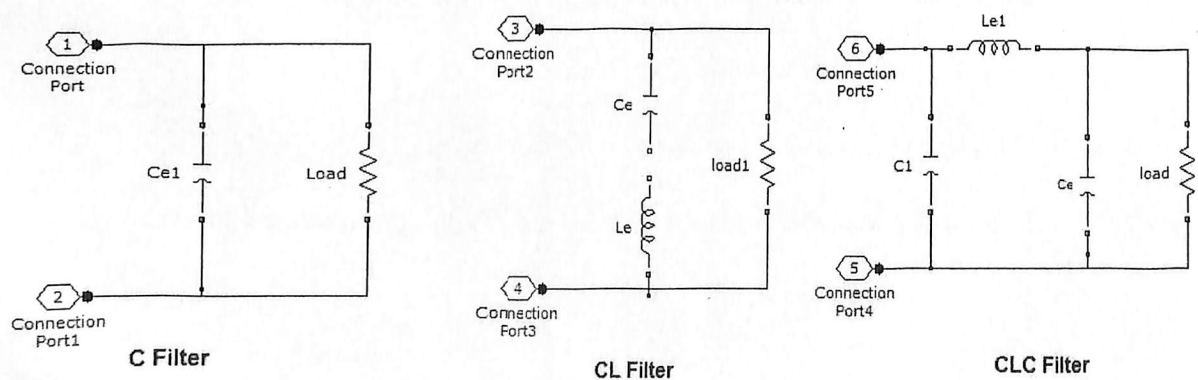
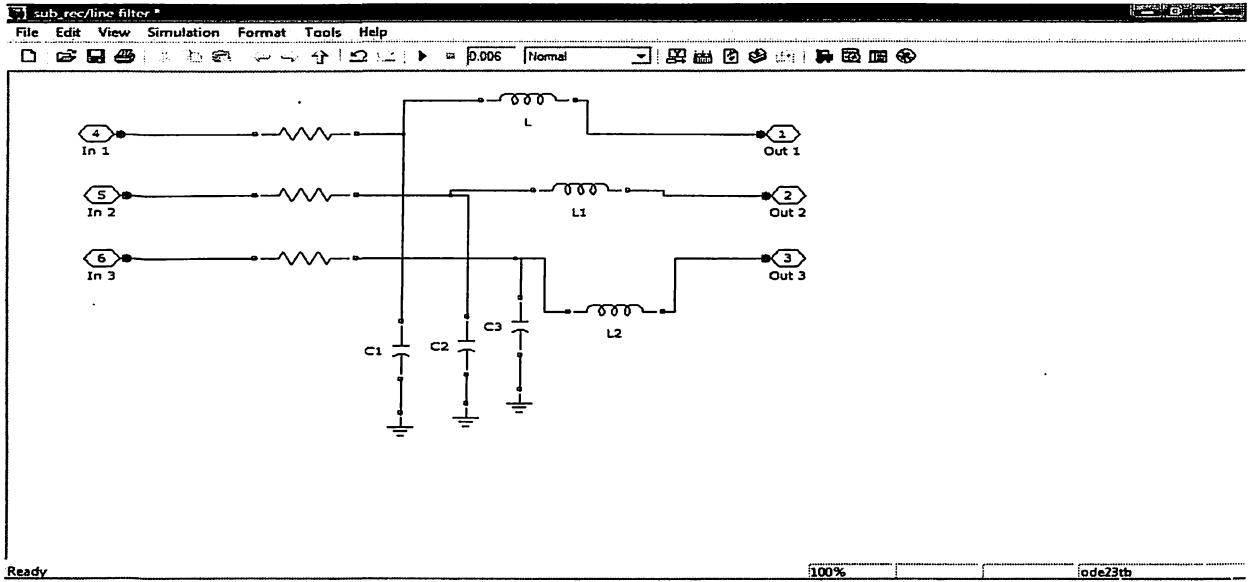


Fig. 4.11 Output Filters



A filter used in the model is CL type which is shown in Fig. 4.12 below.



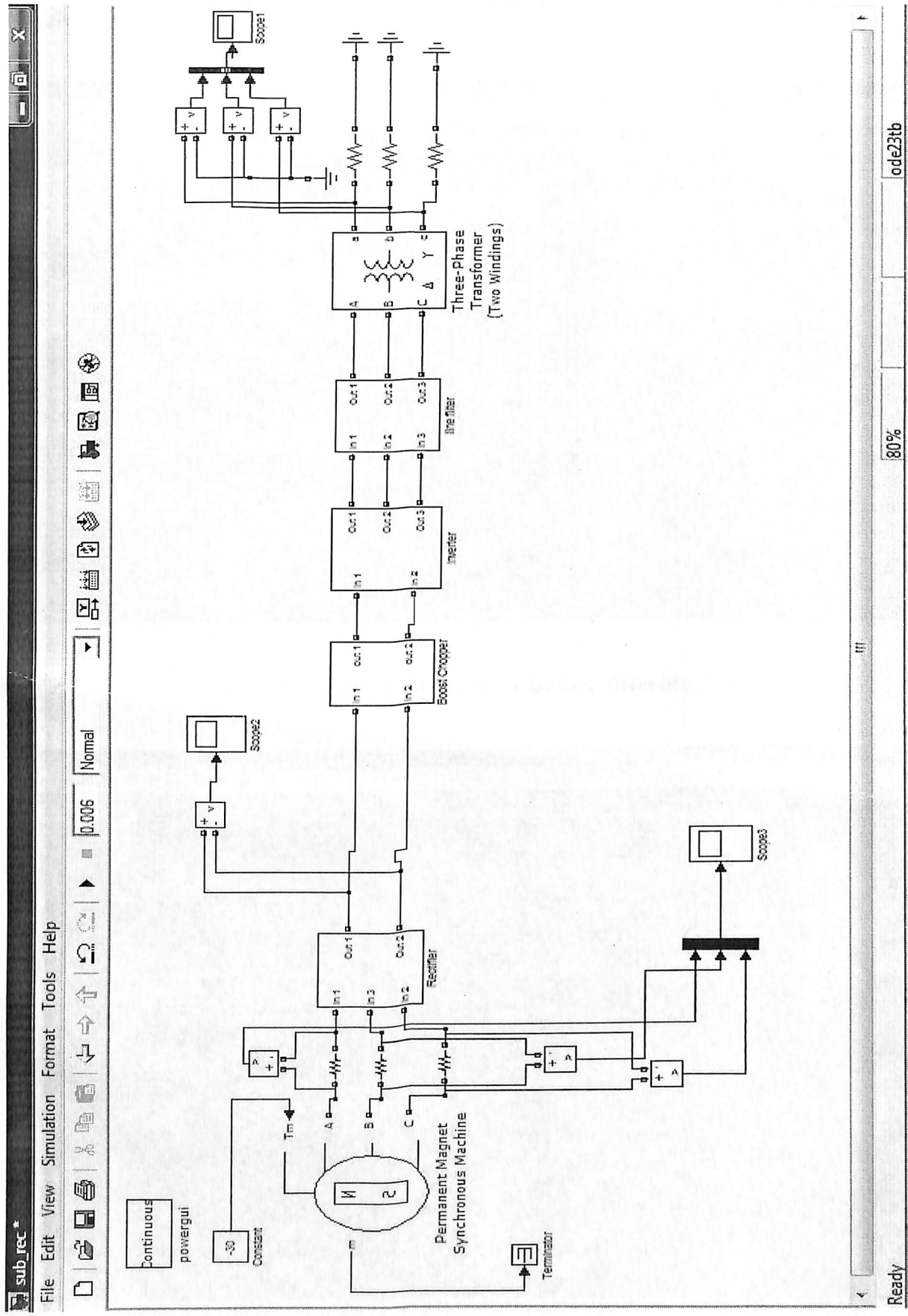
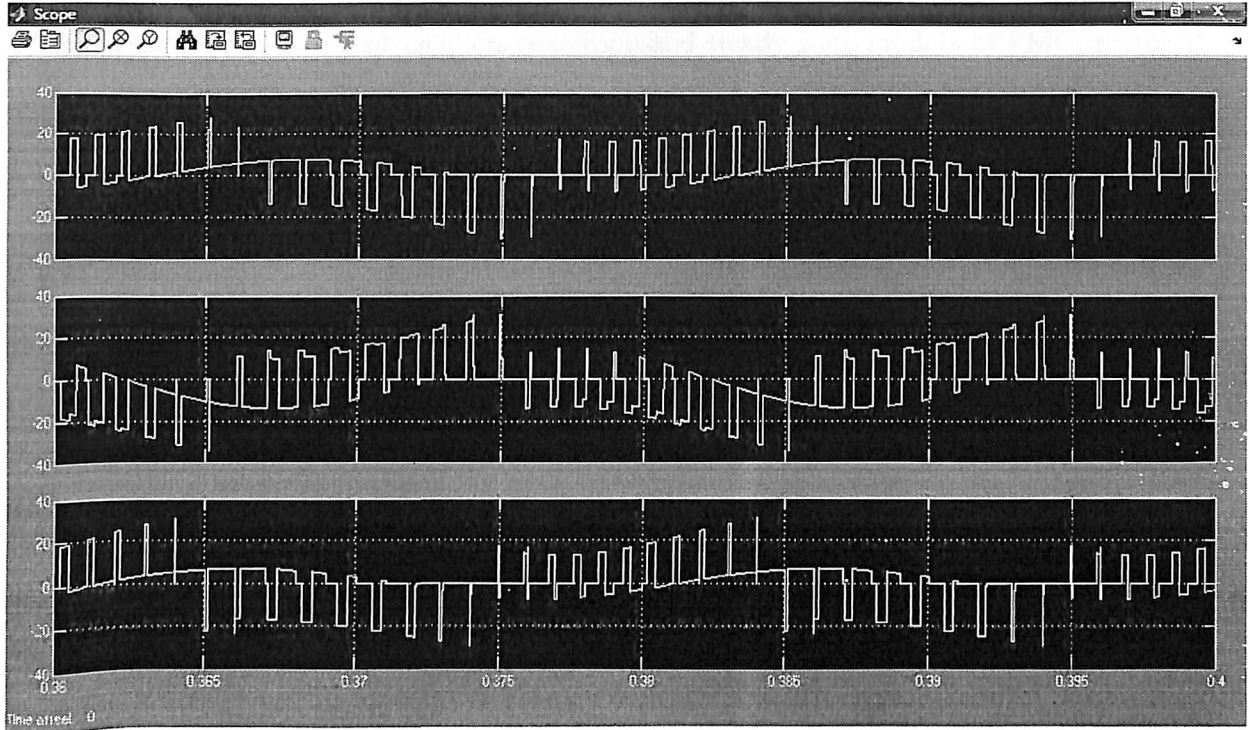
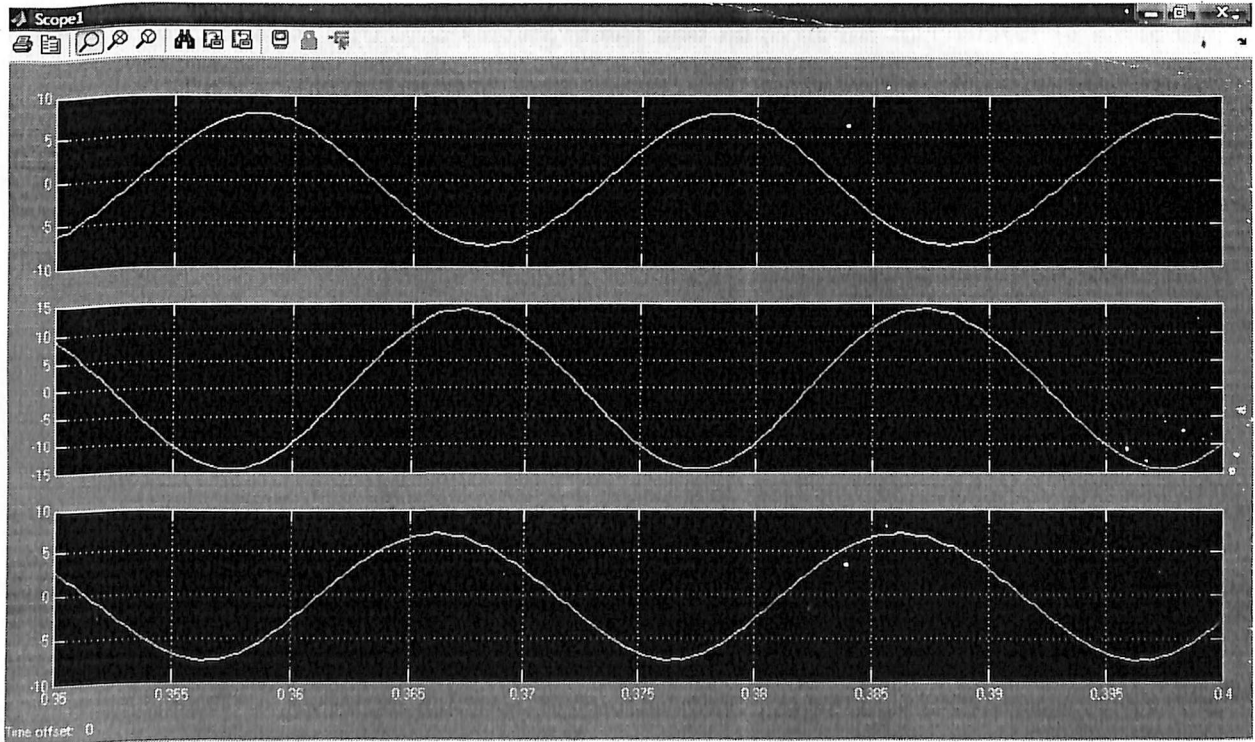


Fig. 4.13 Complete model of PMG

**Results:**



**Fig. 4.14 Output of the inverter before filtering**



**Fig. 4.15 Output of the inverter after filtering**

## CONCLUSION

In this report, with different chapters, we discussed steady state models of PMG, rectifier and inverter; which lead us to understand the working characteristics of PMG base small scale wind power generation. We discussed control scheme of three-phase off-grid wind energy conversion system. The control incorporates for optimal use of wind resource. A three-level voltage source inverter (VSI) is used as interface with the ac load. Validation of models and control schemes is performed by using the MATLAB/Simulink.

Wind energy generation is most relevant solution for future trend power generation, which involving a wide perspective of concern. It has been structured: Identifying first the general improvements and objectives that wind energy generation must address in the future. Then, many technological advantages and possibilities that can contribute to achieve those objectives.

However, future wind turbine technology must also innovate the mechanical structure of the wind turbine itself, guarantee increasing penetration into the market with effective and reliable grid interconnection, widen the location of the wind turbines by developing their capacities, and increasing diversification while paying attention to environmental concerns.

Consequently, in order to optimize wind turbine technology in a more efficient and reliable way, it is necessary to coordinate the innovation efforts, yielding a more integrated design. At the same time the application itself must be considered, together with all the elements of the wind turbine: the electric generator, the converter, the gear, the mechanical structure, the aerodynamic, the location, grid integration, and so on.

## References:

- 1) "MATLAB and Simulink for Engineers", Agam Kumar Tyagi, Oxford University Press 2012.
- 2) "A New Strategy of Variable Speed Wind Turbine Generator for Three-Phase Grid-Connected Applications", M. G. Molina, Member, *IEEE* and P. E. Mercado, Senior Member, *IEEE*.
- 3) "Modeling and Simulation of Wind Turbine Driven Permanent Magnet Generator with New MPPT Algorithm", R. Bharanikumar, A.C. Yazhini, A. Nirmal Kumar.
- 4) "11<sup>th</sup> National Training Course on Wind Energy Technology 28<sup>th</sup> to 30<sup>th</sup> Dec 2011", Centre For Wind Energy Technology, Chennai.
- 5) "Power Electronics, converters, applications, and design", Ned Mohan, Tore M. Undeland, William P. Robbins.
- 6) "Power Electronics, Circuits, Devices, and Applications", Third Edition, Muhammad H. Rashid.
- 7) <http://www.wind-energy-the-facts.com/>.
- 8) <http://www.windplatform.eu/>.
- 9) European wind Energy Association, available at [www.ewea.org](http://www.ewea.org).
- 10) International Energy Agency Wind, Available at <http://www.ieawind.org/>.
- 11) Renewable Energy database, available at <http://www.re-database.com/>.
- 12) <http://www.thewindpower.net>.
- 13) <http://www.gwec.net/>
- 14) [www.retscreen.net](http://www.retscreen.net)

## APPENDIX

### Matlab coding for Fig. 1.2:

```

%%%%% Plot for power output v/s wind speed %%%%%
wind_speed = 3:1:17;
power_2 = [0 0.3 0.6 1.8 2.6 3.5 4.9 6.4 7.7 9.2 10 10 10 5.5 2.8];
plot(wind_speed,power_2,'bo-');
grid;
ylim([0 11]);
xlabel('Wind Speed (m/s)');
ylabel('Power output (kW)');
gtext('<----- Cut-in Speed');

```

### Matlab coding for Fig. 1.3:

```

wind_speed = 3:1:17;
power_1 = [0 44 135 261 437 669 957.9 1279 1590 1823 1945 1988 2000 2000 2000];
plot(wind_speed,power_1,'ks-');
grid;
ylim([0 2200]);
xlabel('Wind Speed (m/s)');
ylabel('Power Output (kW)');
gtext('<-----Cut-in Speed');

```

**Matlab coding for Fig. 1.4:**

```
wind_speed = 3:1:17;
```

```
Cp = [0 0.228 0.358 0.401 0.422 0.433 0.435 0.424 0.396 0.350 0.294 0.240 0.196 0.162  
0.135];
```

```
plot(wind_speed,Cp,'ko-');
```

```
grid;
```

```
xlabel('Tip Speed Ratio');
```

```
ylabel('Power Coefficient Cp');
```